

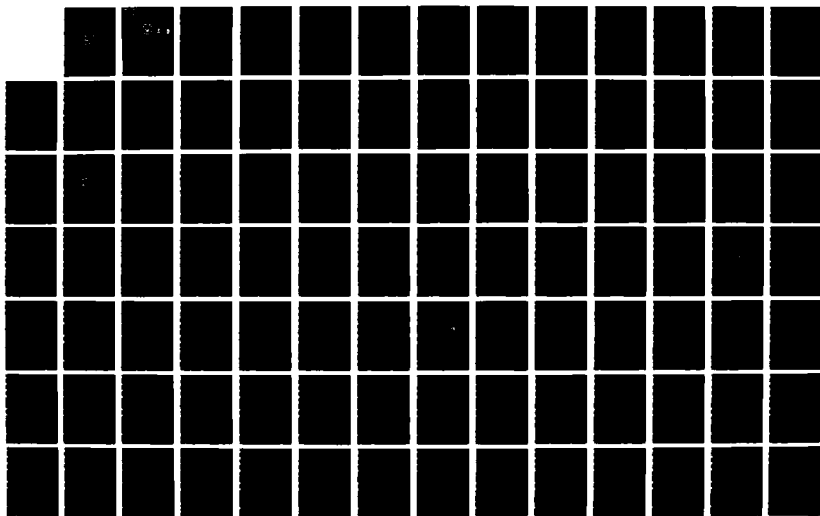
AD-R187 179

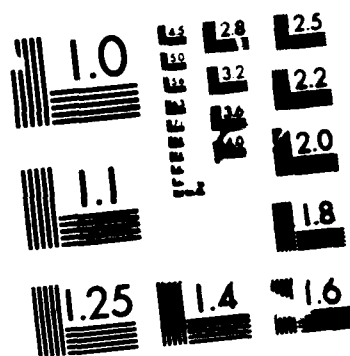
PRELIMINARY DESIGN OF THE ORION ATTITUDE CONTROL SYSTEM 1/2
(U) NAVAL POSTGRADUATE SCHOOL MONTEREY CA D C CHAPPELL
DEC 87

UNCLASSIFIED

F/G 22/2

NL





MICROCOPY RESOLUTION TEST CHART
NATIONAL BUREAU OF STANDARDS-1963-A

AD-A187 179

NAVAL POSTGRADUATE SCHOOL

Monterey, California



DTIC
ELECTE
DEC 14 1987
S D
CED

THESIS

PRELIMINARY DESIGN OF THE ORION
ATTITUDE CONTROL SYSTEM

by

David C. Chappell

December 1987

Thesis Advisor:

G. Thaler

Approved for public release; distribution is unlimited

UNCLASSIFIED

SECURITY CLASSIFICATION OF THIS PAGE

AD-A187179

REPORT DOCUMENTATION PAGE

1a REPORT SECURITY CLASSIFICATION UNCLASSIFIED			1b RESTRICTIVE MARKINGS		
2a SECURITY CLASSIFICATION AUTHORITY			3 DISTRIBUTION/AVAILABILITY OF REPORT Approved for public release; distribution is unlimited		
2b DECLASSIFICATION/DOWNGRADING SCHEDULE			4 PERFORMING ORGANIZATION REPORT NUMBER(S)		
6a NAME OF PERFORMING ORGANIZATION Naval Postgraduate School			6b OFFICE SYMBOL (if applicable) Code 62		7a NAME OF MONITORING ORGANIZATION Naval Postgraduate School
6c ADDRESS (City, State, and ZIP Code) Monterey, California 93943-5000			7b ADDRESS (City, State, and ZIP Code) Monterey, California 93943-5000		
8a NAME OF FUNDING/SPONSORING ORGANIZATION		8b OFFICE SYMBOL (if applicable)		9 PROCUREMENT INSTRUMENT IDENTIFICATION NUMBER	
8c ADDRESS (City, State, and ZIP Code)		10 SOURCE OF FUNDING NUMBERS			
		PROGRAM ELEMENT NO	PROJECT NO	TASK NO	WORK UNIT ACCESSION NO
11 TITLE (Include Security Classification) PRELIMINARY DESIGN OF THE ORION ATTITUDE CONTROL SYSTEM					
12 PERSONAL AUTHOR(S) Chappell, David C.					
13a TYPE OF REPORT Master's Thesis		13b TIME COVERED FROM _____ TO _____		14 DATE OF REPORT (Year, Month, Day) 1987, December	
15 PAGE COUNT 100					
16 SUPPLEMENTARY NOTATION					
COSATI CODES			18 SUBJECT TERMS (Continue on reverse if necessary and identify by block number)		
FIELD	GROUP	SUB-GROUP	Attitude Control System; ORION		
19 ABSTRACT (Continue on reverse if necessary and identify by block number)					
<p>This thesis models the motion of the NPS satellite ORION using the three Euler rotation angles. The simulation program also models aerodynamic drag and gravity gradient torques. Simulations are performed to analyze the effect of changing the inertia ratio on satellite stability and performance. The active nutation control method was also simulated and an example of its operation given. The amount of time required to reduce nutation to an acceptable level was found to be dependent on the initial nutation angle, spin rate, and thruster size. The slower the spin rate, the greater the torque that could be</p>					
20 DISTRIBUTION/AVAILABILITY OF ABSTRACT <input checked="" type="checkbox"/> UNCLASSIFIED UNLIMITED <input type="checkbox"/> SAME AS RPT <input type="checkbox"/> DTIC USERS			21 ABSTRACT SECURITY CLASSIFICATION Unclassified		
22a NAME OF RESPONSIBLE INDIVIDUAL Prof. George Thaler			22b TELEPHONE (Include Area Code) (408) 646-2134		22c OFFICE SYMBOL Code 62Tr

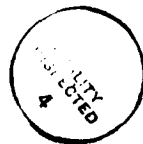
UNCLASSIFIED

SECURITY CLASSIFICATION OF THIS PAGE (When Data Entered)

#19 - ABSTRACT - (CONTINUED)

used during a given firing arc resulting in faster
mutation control.

Accession For	
NTIS	<input checked="checked" type="checkbox"/>
DA	<input type="checkbox"/>
DTIC	<input type="checkbox"/>
DTIC	<input type="checkbox"/>
Availability Codes	
All and/or Special	
A-1	



UNCLASSIFIED

SECURITY CLASSIFICATION OF THIS PAGE (When Data Entered)

Approved for public release; distribution is unlimited

Preliminary Design of the ORION
Attitude Control System

by

David C. Chappell
Lieutenant, United States Navy
B.S., University of Kansas, 1979

Submitted in partial fulfillment of the
requirements for the degree of

MASTER OF SCIENCE IN ELECTRICAL ENGINEERING


from the

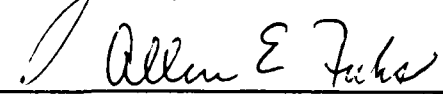
NAVAL POSTGRADUATE SCHOOL
December 1987


Author:



David C. Chappell

Approved by:


G. Thaler, Thesis Advisor


A.E. Fuhs, Second Reader


J. Powers, Chairman
Department of Electrical
and Computer Engineering


Gordon E. Schacher,
Dean of Science and Engineering

ABSTRACT

➤ This thesis models the motion of the NPS satellite ORION using the three Euler rotation angles. The simulation program also models aerodynamic drag and gravity gradient torques. Simulations are performed to analyze the effect of changing the inertia ratio on satellite stability and performance. The active nutation control method was also simulated and an example of its operation given. The amount of time required to reduce nutation to an acceptable level was found to be dependent on the initial nutation angle, spin rate, and thruster size. The slower the spin rate, the greater the torque that could be used during a given firing arc resulting in faster nutation control. ←

TABLE OF CONTENTS

I.	CONTROL SYSTEM OVERVIEW -----	10
	A. LAUNCH -----	17
	B. ATTITUDE ACQUISITION -----	18
	C. MISSION -----	21
	D. ASSUMPTIONS -----	21
II.	ATTITUDE SENSORS -----	26
	A. SUN SENSORS -----	26
	B. HORIZON SENSORS -----	28
	C. MAGNETOMETERS -----	32
	D. NUTATION -----	33
III.	ATTITUDE DYNAMICS AND CONTROL -----	35
	A. ATTITUDE DYNAMICS -----	35
	B. ENVIRONMENTAL TORQUES -----	45
	C. COMPUTER MODEL -----	48
IV.	PARAMETER STUDIES AND ACQUISITION SIMULATION ---	50
	A. SIMULATION MODEL -----	50
	B. PARAMETER STUDIES -----	50
	C. ENVIRONMENTAL EFFECTS -----	60
	D. ACQUISITION PHASE PROFILE -----	66
V.	MISSION PHASE SIMULATION -----	69
	A. SATELLITE CONTROL -----	69
	B. SATELLITE REORIENTATION -----	86
VI.	CONCLUSIONS -----	92

APPENDIX: ATTITUDE ANGLE CONTROL PROGRAM -----	95
LIST OF REFERENCES -----	98
INITIAL DISTRIBUTION LIST -----	99

LIST OF TABLES

1.1	ATTITUDE CONTROL METHOD COMPARISONS -----	13
1.2	ATTITUDE CONTROL METHOD APPLICATIONS -----	15
3.1	ROOTS OF THE TRANSFER FUNCTION -----	45
4.1	TYPICAL VALUES FOR AERODYNAMIC DRAG -----	60

LIST OF FIGURES

1.1	ORION Diagram -----	11
1.2	Attitude Control Block Diagram -----	16
1.3	Initial Axes Orientation and Attitude Angles ----	20
1.4	Attitude Control Algorithm -----	22
2.1	Sun Sensor Schematic -----	27
2.2	Horizon Sensor Location -----	30
2.3	Relationship Between Earth Chord and Roll Angle -	31
3.1	System Block Diagram -----	41
3.2	Nutation Cone -----	43
4.1	Magnetometer Deployment Diagram -----	52
4.2	Change in Moments of Inertia with Boom Length ---	54
4.3	Change in Spin Rate with Magnetometer Deployment -----	55
4.4	The Effects of Inertia Ratio on Nutation Frequencies -----	58
4.5	Satellite Response to a Short Duration Torque -----	59
4.6	Nutation Angles for Different Spins and Inertias -----	61
4.7	Nutation Due to Environmental Torques; 10 RPM ---	63
4.8	Nutation Due to Environmental Torques; 20 RPM ---	64
4.9	Nutation Due to Environmental Torques; 60 RPM ---	65
4.10	Acquisition Phase Roll and Yaw -----	67
5.1	Typical Thruster Profile (Trapezoid Model) -----	71
5.2	Relationship Between Spin Rate and Firing Times -----	73

5.3	Nutation Control; $\omega_y = 10$ RPM -----	77
5.4	Roll and Yaw Angles; $\omega_y = 10$ RPM -----	78
5.5	Firing Diagram; $\omega_y = 10$ RPM -----	79
5.6	Nutation Control; $\omega_y = 20$ RPM -----	80
5.7	Roll and Yaw Angles; $\omega_y = 20$ RPM -----	81
5.8	Firing Diagram; $\omega_y = 20$ RPM -----	82
5.9	Nutation Control; $\omega_y = 60$ RPM -----	83
5.10	Roll and Yaw Angles; $\omega_y = 60$ RPM -----	84
5.11	Firing Diagram; $\omega_y = 60$ RPM -----	85
5.12	Nutation Variation with σ ; $\omega_y = 20$ RPM -----	87
5.13	Relationship Between ω_y , λ , and ω_n -----	90

I. CONTROL SYSTEM OVERVIEW

This thesis is intended to act as the preliminary ground work for the attitude control system of the Naval Postgraduate School satellite ORION. The background for ORION is detailed in Reference 1. The orbital control system deals with the motion of the center of mass in an orbit around the earth, while the attitude control system deals with the angular motion of a satellite around its center of mass. The attitude control system must incorporate attitude sensors, control laws, actuators or thrusters, the effect of disturbing forces and the dynamics of the satellite.

ORION is being designed to be launched via the extended Get-Away-Special (GAS) cannister aboard the Space Transportation System (Space Shuttle). ORION is currently under development and many of the systems which will determine its final characteristics have not been fixed. For the purpose of this thesis, ORION is considered to be a cylindrical satellite of uniform mass with dimensions of 0.889 meters height and 0.4826 meters diameter. It has a mass of 113 kilograms. Figure 1.1 shows a diagram of ORION.

The design of a control system is highly dependent on the mission of the satellite. Reference 2 provides a section on the analysis of mission requirements and the

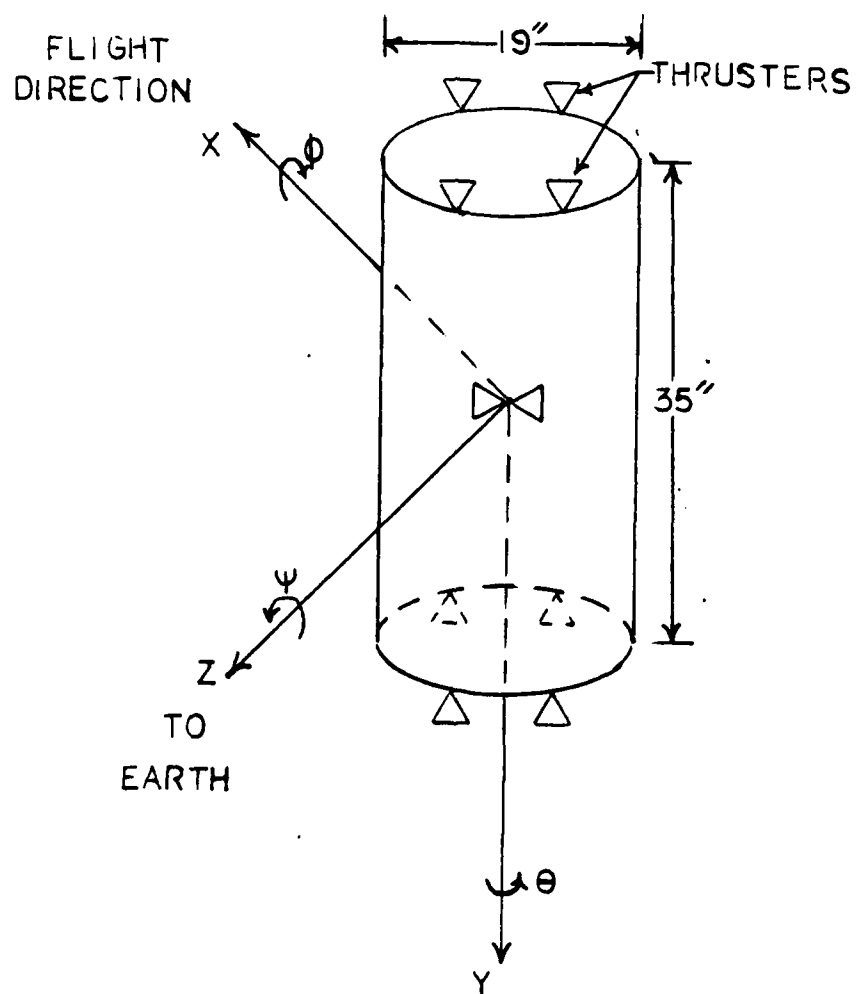


Figure 1.1 ORION Diagram

possible control systems which will fulfill mission requirements. Tables 1 and 2 show the trade-offs that need to be made when choosing a type of control system [Ref. 2:pp. IV-12,IV-12].

ORION is being designed to act as a payload bus for a variety of missions. General requirements are that the satellite fly in orbits from 200 kilometers to 2000 kilometers. Attitude sensor accuracies will not be less than 2.0 degrees. The life of the satellite will depend on a mission payload versus fuel trade-off. For missions that do not require a high degree of pointing accuracy, spin stabilization provides the simplest means of attitude control. A spinning satellite will be less susceptible to nutation if spun about a maximum moment of inertia and will be stable if energy can be dissipated. The equations governing satellite motion are developed in Chapter III.

The purpose of the control system is to maintain the satellite at a specified orientation in space. If the satellite is perturbed from this orientation by external factors such as gravity gradient torques, aerodynamic drag or nutation then the control system must sense the change and apply the control torques necessary to reorient the satellite. It must also be able to reorient the satellite to accommodate any change in the mission requirements. Figure 1.2 shows a diagram of the basic control system. The feedback loop and error determination process may occur

TABLE 1.1

ATTITUDE CONTROL METHOD COMPARISONS

<u>System Types</u>	<u>Advantages</u>	<u>Disadvantages</u>
<u>Mass Expulsion (Pneumatic) Systems</u> Utilize gas jets in closed loop control system employing attitude sensors.	<ul style="list-style-type: none"> - Insensitive to disturbance torques. - Provides widest variety of control orientations. - Precision limited to that of attitude sensor. 	<ul style="list-style-type: none"> - Becomes quite heavy for long missions when used alone. - Require attitude sensors.
<u>Momentum Storage Devices</u> Power driven reaction wheels, gyros or fluid loops which absorb or impart limited angular momentum to vehicle.	<ul style="list-style-type: none"> - Relieve gas system fuel expenditure for long missions. - Very precise nulling control. - Precision limited only by attitude or sighting sensors. 	<ul style="list-style-type: none"> - Requires auxiliary gas system to unload momentum saturation. - Increased system complexity and power consumption.
<u>Gravity Gradient Systems</u> The difference in the earth's gravity field at the top and bottom ends of the space vehicle creates a torque which aligns vehicle with local vertical. A damper is used to reduce oscillations.	<ul style="list-style-type: none"> - Involves no active control elements. - Requires no attitude sensors. - High reliability. 	<ul style="list-style-type: none"> - Extremely sensitive to environmental torques and payload motion. - Limited to near-circular orbits (eccentricity less than 0.02). - Local vertical accuracy limited from 2 to 3 degrees at 500 miles to 10 degrees at synchronous altitude.
<u>Spin Stabilization</u> Spinning a vehicle about its axis of maximum inertia maintains an inertial orientation in the absence of applied torques (as with a gyroscope).	<ul style="list-style-type: none"> - Fixed inertial orientation with limited accuracy for negligible weight. 	<ul style="list-style-type: none"> - Orientation of more than one axis to a fixed reference requires that part of the vehicle be decoupled from the spinning portion. - Impractical for rapidly rotating line of sight requirements. - Spin speeds reduce 50% each 100 to 200 days.

TABLE 1.1 (CONTINUED)

<u>System Types</u>	<u>Advantages</u>	<u>Disadvantages</u>
<u>Magnetic Systems</u> Electric current loops within the space vehicle produce magnetic fields which align with the earth's magnetic field.	<ul style="list-style-type: none"> - May be achievable with negligible weight. - Requires no attitude sensors. - High reliability. 	<ul style="list-style-type: none"> - Limited to altitudes below 20,000 nautical miles. - Very limited application. - Accuracy limited to a few degrees.

Source: [Ref. 2:p. IV-12]

TABLE 1.2
ATTITUDE CONTROL METHOD APPLICATIONS

Applications	Attitude Control Methods				
	Gravity Gradient	Magnetic Control	Pneumatic Control	*Momentum Storage	Spin Stabilization
Manned Vehicles	No		Yes	Yes	No
Earth Orientation	Yes	Yes	Yes	Yes	No
Inertial Orientation	No		Yes	Yes	Yes
Earth/Sun Orientation			Yes	Yes	No
Powered Flight Control	No	No	Yes		Yes
Precise Station Keeping			Yes	Yes	Yes
Orbit Correction Control	No	No	Yes		Yes
Vehicle Slewing	No	No	Yes	Yes	No
100 to 300 Mile Orbits	No		Yes	Yes	No
300 to 20,000 Mile Orbits	Yes	Yes	Yes	Yes	Yes
20,000 Mile - Orbits	No	No	Yes	Yes	Yes
1 to 10 Degree Accuracy	Yes	Yes	Yes	Yes	Yes
0.2 to 2.0 Degree Accuracy	No	Yes	Yes	Yes	Yes
0.01 to 0.2 Degree Accuracy	No		Yes	Yes	
0.1 Arc-Seconds-0.01 Degree Accuracy	No	No		Yes	No
Fast Response Time	No	No	Yes	Yes	
*Momentum storage devices cannot be used without an auxiliary torque producing system	Legend Yes - Can be used No - Cannot be used Blank - Will not provide this function alone but may be used				

Source: [Ref. 2:p. IV-12]

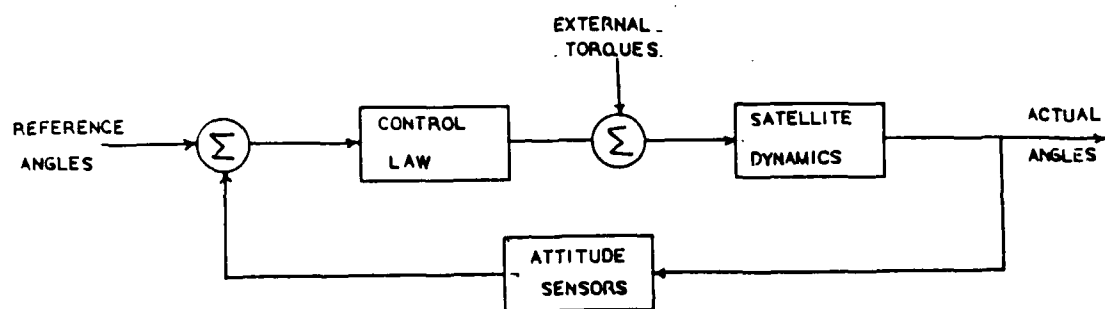


Figure 1.2 Attitude Control Block Diagram

either on board the satellite or via a satellite to earth station telemetry link. On-board processing requires preprogramming the reference angles into the processor and is limited to those periods when the control system needs to act only as a regulator and any disturbances are small. A telemetry link is required to control the satellite during major orientation periods and flight maneuvers. It also acts as a back-up for the on board processor.

There are three distinct phases of the attitude control problem. They are: 1) launch, consisting of activities required to take the satellite into a preliminary orbit; 2) acquisition, in which the satellite's preliminary orientation and maneuvers are accomplished; and 3) mission operations, in which the mission requirements are carried out [Ref. 3:p. 12].

A. LAUNCH

Control during launch is limited to the launch vehicle and has little relationship to the attitude control of the satellite. Of primary concern is the detachment of the satellite from the launch vehicle in some preliminary orbit. The satellite will have the angular momentum of the launch vehicle plus some velocity imparted from the separation process. ORION will be carried into orbit by the Space Shuttle and launched from a GAS cannister. Reference 1 details the cannister and the launch process. The launch

vector is along an outward radial from Earth's center at 4 feet per second.

B. ATTITUDE ACQUISITION

The acquisition phase commences after ORION is detached from the Shuttle. During this phase the control problem consists of determining the attitude of the satellite, spinning the satellite up to the desired spin rate, reorienting the satellite to align the maneuvering thruster with the velocity vector required to place the satellite in its mission orbit and maintaining the correct attitude during the orbit transfer. Once in its final orbit, the control system must reorient the satellite to the desired mission attitude.

NASA prohibits the firing of thrusters over 5 pounds sooner than 45 minutes after separation. Thrusters under 5 pounds cannot be fired closer than 200 feet to the shuttle. At a launch velocity of 4 feet per second, this means the satellite will drift for 50 seconds before beginning spin up for attitude orientation. During this drift time the primary forces acting on the satellite are aerodynamic drag and gravity gradient torque. Additional torques will be present if the satellite contacts the cannister side during the launch process. The environmental torques are developed in Chapter III.

The attitude of the satellite can be predicted during the drift period by applying these torques to the basic

satellite equations of motion. Some assumptions must be made concerning the initial conditions at the time of launch. These are:

- (1) The satellite does not impact the cannister during the launch process. If this happens the satellite will tumble and the attitude cannot be predicted. The motion would have to be observed by the Shuttle crew and reported.
- (2) The satellite is aligned as shown in Figure 1.3 with the z axis pointing towards the earth and the x axis in the direction of flight. The initial values of ϕ , ψ and θ are zero.
- (3) The aerodynamic drag force acts only against the satellite's center of pressure and opposite to the direction of flight.

After the satellite is 200 feet from the shuttle, it is spun up to 60 rpm and the actual attitude determined by the horizon and sun sensors. A description of the horizon and sun sensors is given in Chapter II. Once the orientation of ORION is determined, control torques may be applied to orient it to any desired attitude. During this time system tests may be performed to verify the correct operation of the satellite. Details concerning control torques are found in Chapter III.

The next portion of the acquisition phase is to orient ORION for orbital maneuvering. It is unlikely that the Shuttle will be able to launch ORION into its final orbit. For its first mission ORION will be required to extend four magnetometers from the body. This deployment will have two major effects. It will despin the satellite and it will increase the moments of inertia about the spin and

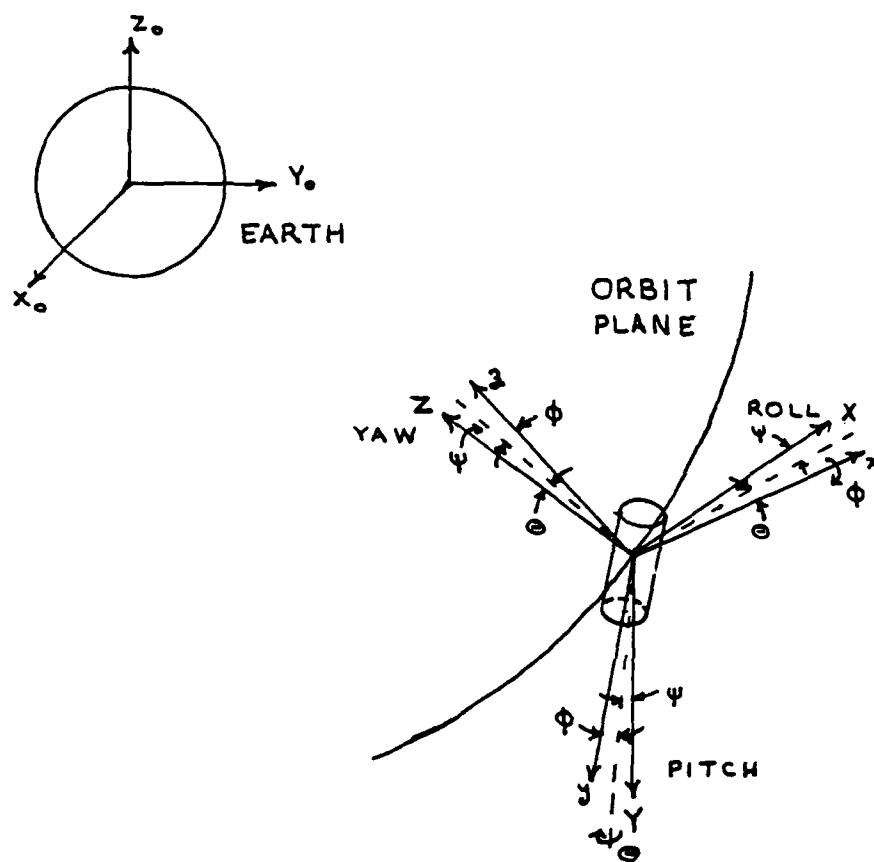


Figure 1.3 Initial Axes Orientation and Attitude Angles

transverse axes. Once the magnetometers are deployed, the satellite will need to be oriented to align the propulsion thruster with the velocity vector which will maneuver ORION into its final orbit. Details on the final orbit are not yet available.

C. MISSION

The third phase of the attitude problem is the control of the satellite while it is performing its mission. Generally this requires the control system to act as a regulator to maintain the correct orientation. If the required attitude is fixed, the control loop may be programmed into a micro-processor and function autonomously. The telemetry link would be used to monitor the processor and act as a back-up. Control by the earth station may be necessary to orient the satellite for maneuvers or to correct for a large disturbance. Figure 1.4 summarizes the control problem in algorithmic form.

D. ASSUMPTIONS

The purpose of this thesis is to form a model of ORION and simulate its motion during the three phases of the control problem. It will model the satellite's equations of motion, the environmental disturbance torques, and the control torques and study the interactions between these factors. As stated earlier, ORION is still in the early stages of design. Many of the systems which determine the

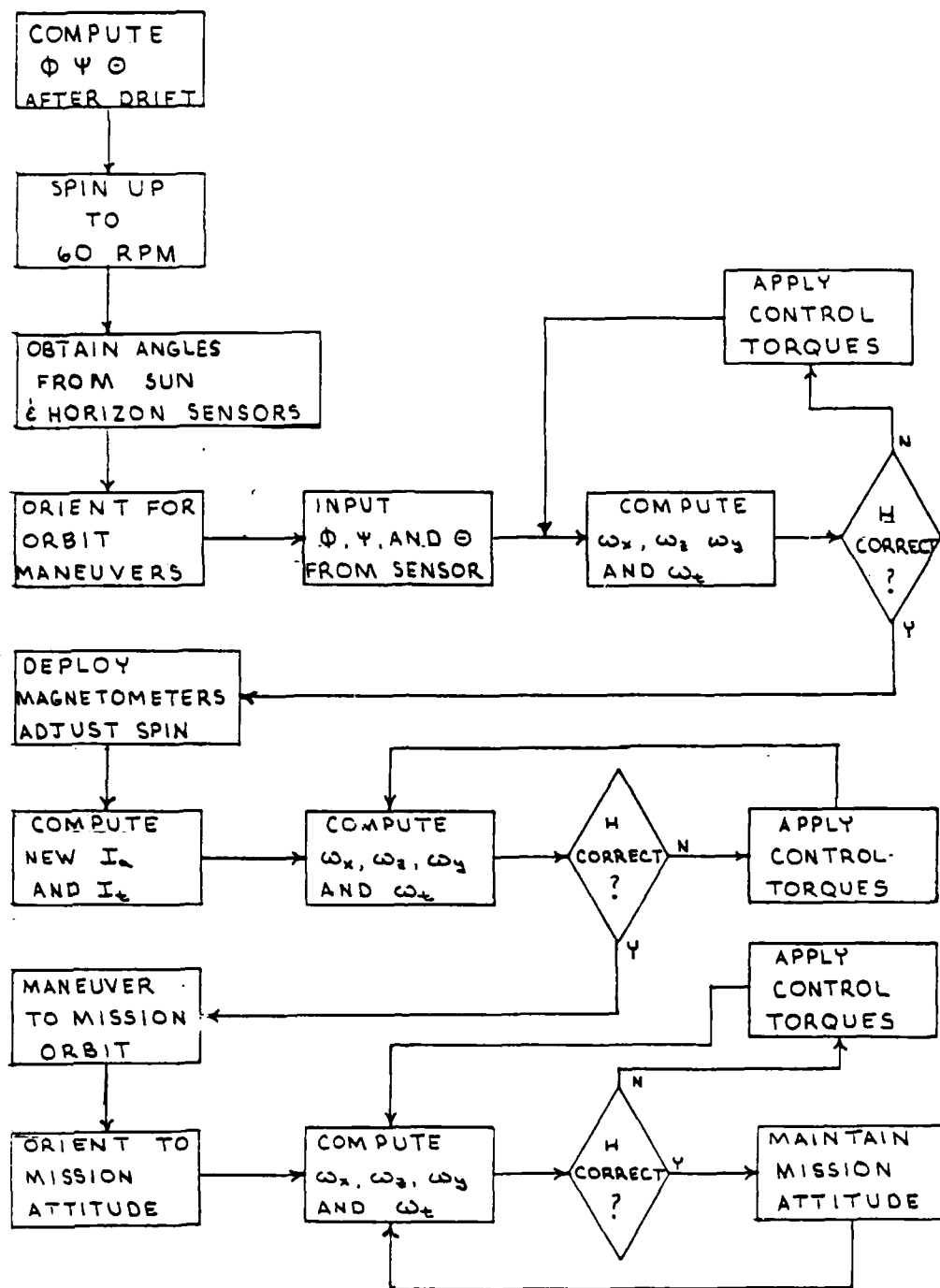


Figure 1.4 Attitude Control Algorithm

flight characteristics have not been developed. It is necessary therefore to make a number of assumptions which simplify the simulation problem. As the design of ORION matures assumptions may be removed and the model updated. This will help in determining design trade-offs and increase the accuracy of the model.

The first major assumption is that the satellite has a uniformly distributed mass. This locates the center of mass at the origin of the body aligned axis as shown in Figure 1.1. The moments of inertia are dependent on the deployment of the magnetometers, but in the launch configuration I_a is 3.239 kg-m^2 and I_t is 8.916 kg-m^2 . As the mass distribution changes because of component location or changes in fuel weight, payload, etc., these moments of inertia will change. If the moments of inertia are located along the body aligned axes, the cross products of inertia are zero. The second major assumption is that the orbit will be circular. This results in a constant angular velocity ω_0 around the earth. The radius of orbit also remains constant throughout the orbit.

The model of the satellite will first be constructed assuming the satellite is a rigid body with no internal energy effects such as sloshing fuel tanks. It will also be assumed that there will be no significant changes in the moments of inertia because of the control thruster burns.

Energy effects can be taken into account later in the simulation process.

The model will also assume that the spin rate of the satellite will remain constant. In actuality the drag force on the satellite will cause the spin rate to decrease significantly in approximately 50 days [Ref. 4:p. 34]. This will be ignored in the model since if a significant reduction is noticed, then the spin thrusters can easily be fired to spin the satellite without affecting the orientation.

When a satellite is in orbit, it is subjected to a variety of environmental forces and moments. These environmental disturbances include gravity gradient torque, aerodynamic drag, solar radiation pressure, magnetic field torques and micrometeor and radiation impacts. Gravity gradient and aerodynamic drag effects are dependent on the radius of the orbit. As the radius increases these effects are decreased. Solar pressure and magnetic torques are important over a long period of time, but can be ignored when looking at the short term motions. The primary effect of these environmental disturbances is noticed in the nutation and precession of the spinning satellite over time. This model will assume that the total torque on the satellite will be the sum of gravity gradient torque, aerodynamic drag torque and applied control torques. The

model will allow any additional torques to be applied at the simulator's discretion.

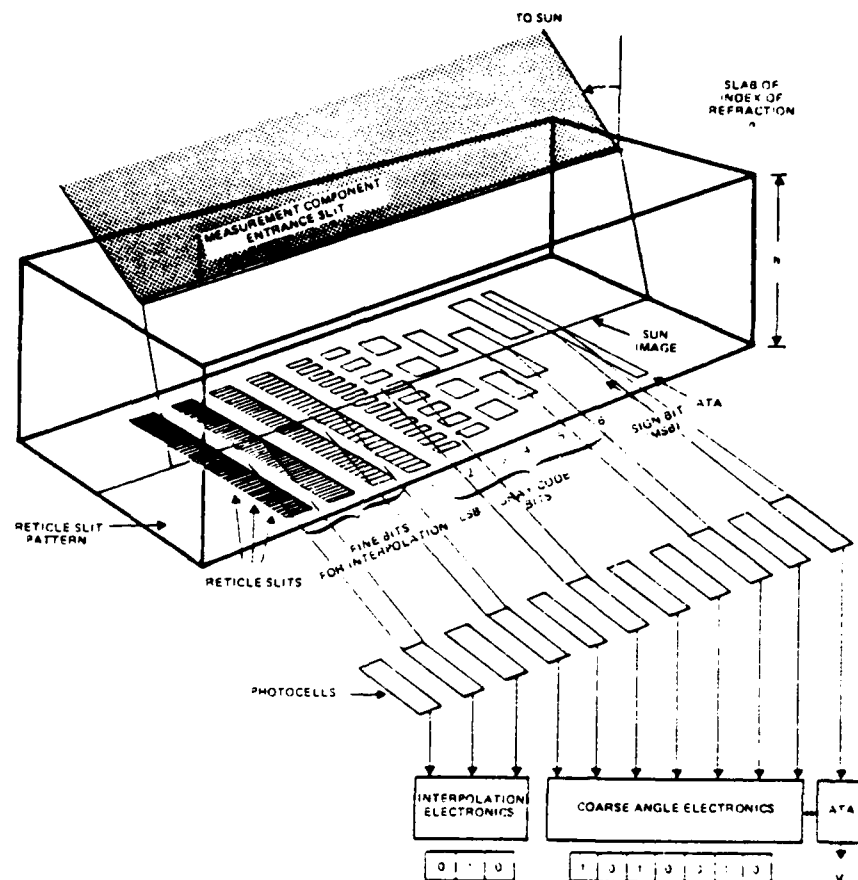
II. ATTITUDE SENSORS

Before control can be applied to a satellite, the actual orientation in space must be determined. This is done by the attitude sensor package. Many devices and methods can be used as attitude sensors. These include rate gyroscopes, star sensors, sun sensors, earth limb or horizon sensors, and magnetometers. This chapter will describe how magnetometers, sun sensors and horizon sensors operate. These three types of sensors are currently planned for use in ORION.

A. SUN SENSORS

Sun sensors are used to measure the angle of the sun relative to the spin axis of the satellite. The sensor consists of a pattern of photoelectric cells and a housing that limits the angle at which the sun's rays contact the cells. Figure 2.1 shows a schematic of the sun sensor [Ref. 3:p. 163].

The field of view slit is oriented parallel to the x-z plane and perpendicular to the spin axis. The angle β determines the amount of sunlight on the photo cells which in turn produces a given amount of voltage. As the spin axis moves in inertial space, usually due to a torque, β changes and the voltage from the photo cells changes. The accuracy of the sun sensor is affected by the quality of solar cells



Source: [Ref. 3:p. 163]

Figure 2.1 Sun Sensor Schematic

used, the presence of any highly reflective components of the satellite and the location of the sensor on the body. A typical accuracy is 0.01 degrees [Ref. 3:p. 17]. The rate of change of β is determined by calculating the time rate of change of the output voltage.

Sun sensor data can be used to calculate nutation and to calculate the yaw angle ψ . The method for determining nutation is described later in this chapter. ψ is determined by using information from the sun sensor and the horizon sensors. The motion of the spin axis is a combination of both ϕ and ψ . If ϕ is known from the horizon sensors then for small angles,

$$\psi^2 = \beta^2 - \phi^2 \quad (2.1)$$

and

$$\dot{\psi} = \dot{\beta} - \dot{\phi} \quad (2.2)$$

B. HORIZON SENSORS

Earth limb or horizon sensors are IR sensors with a set field of view that measures the difference in temperature between space and the earth's limb. Space is considered to have a temperature of 4 degrees Kelvin and the Earth has a temperature of 300 degrees Kelvin. As the sensor's field of view sweeps from space onto the earth a pulse is started. The pulse ends as the FOV goes from earth back onto space.

Two sensors are located equidistant from the center line of the satellite as shown in Figure 2.2. As the satellite spins, the two sensors create a pair of pulses as they cross the earth. The pulse width is determined by

$$PW = R/2h\dot{\theta} \quad (2.3)$$

where R is the earth chord length (Figure 2.3), h is the altitude of the satellite and $\dot{\theta}$ is the spin rate of the satellite.

The sensors can determine ϕ , $\dot{\phi}$, and $\dot{\theta}$. The spin rate $\dot{\theta}$ can be computed by measuring the time between successive pulse starts. ϕ is determined by comparing the pulse widths of sensor 1 and sensor 2. When the pulse width of sensor 1 is less than the pulse width of sensor 2, ϕ is positive. When the pulse width of sensor 1 is greater than that of sensor 2, ϕ is negative. This relationship is shown in Figure 2.3. The value of ϕ is computed by comparing the magnitudes of the pulse widths with those of $\phi = 0$ and using the methods in Chapter 11 of Reference 5. $\dot{\phi}$ is determined by comparing the pulse widths of successive pulses over time.

The accuracy of the sensor is dependent on the quality of components, and the presence of infrared sources other than the earth. Masks are used to block the effects of the sun and avoid the saturation of the sensors. The satellite itself may act as a noise source, however shielding and

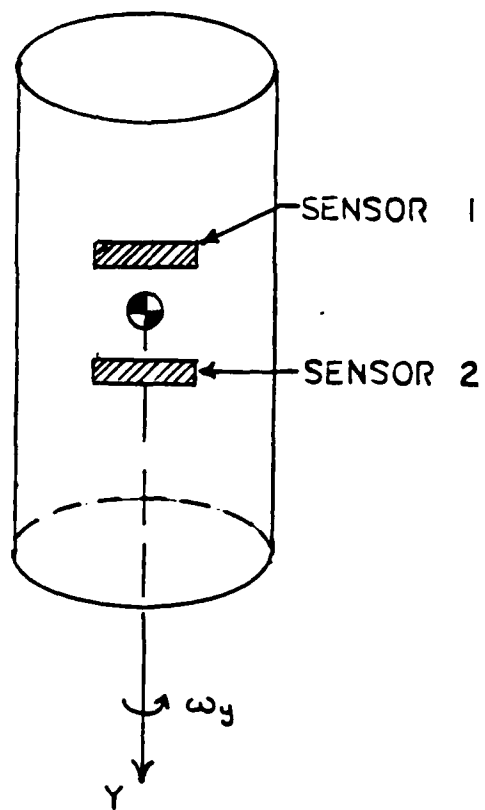


Figure 2.2 Horizon Sensor Location

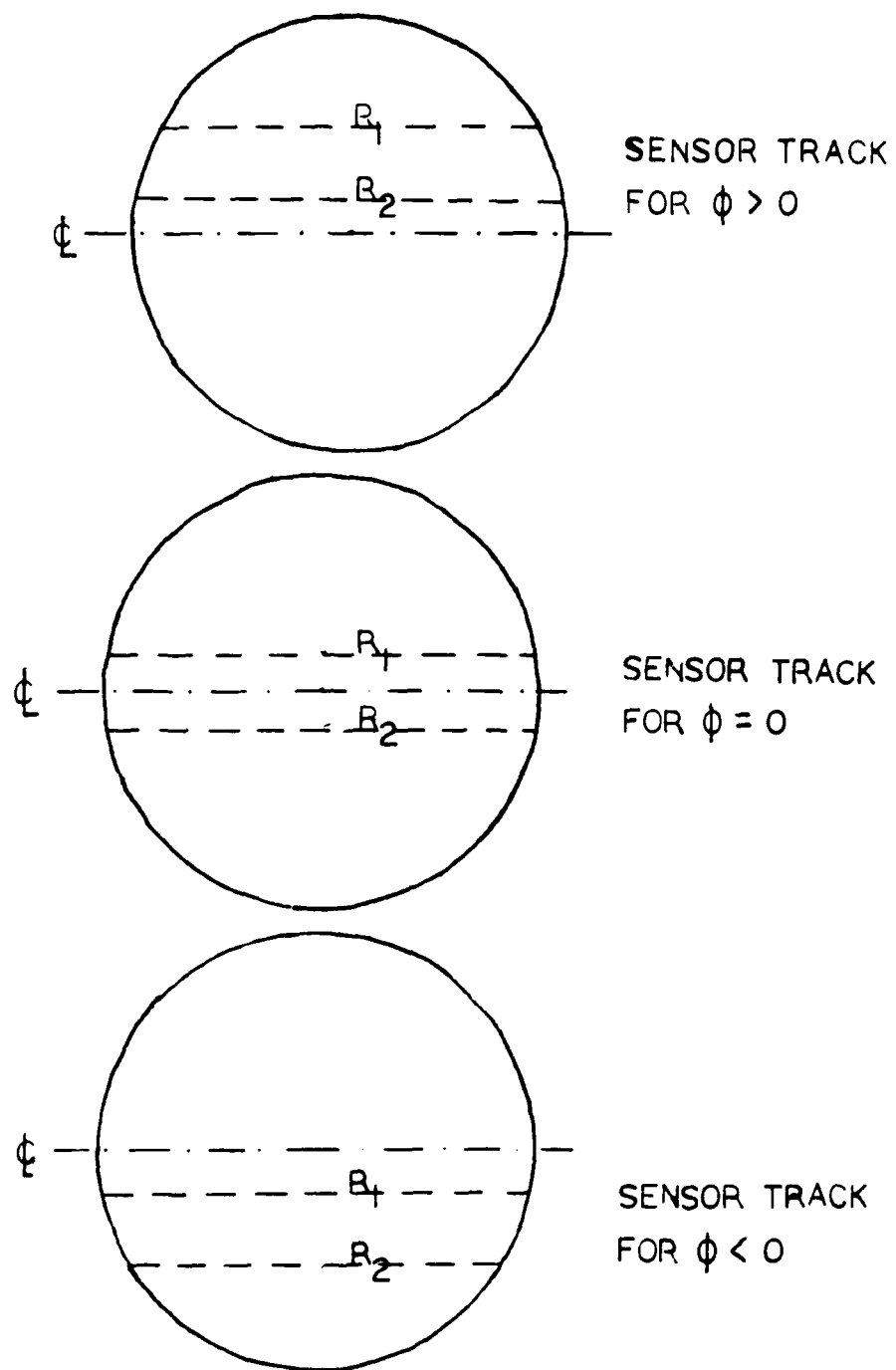


Figure 2.3 Relationship Between Earth Chord and Roll Angle

knowing the infrared signature can reduce the effects. Pages 365-409 of Reference 5 give computational methods used to eliminate errors and determine the accuracy of the sensors. In general the accuracy of a horizon sensor can be assumed to be 0.1 degrees [Ref. 3:p. 17].

C. MAGNETOMETERS

Considering the accuracy in attitude measurements required for ORION, the sun and horizon sensors will suffice for the sensor package. Since magnetometers are going to be used in the mission, they can be used to provide additional attitude inputs. These inputs can be compared with those obtained from the sun and horizon sensors to help eliminate noise and errors in measurements.

For attitude sensing purposes, three mutually orthogonal magnetometers are required. These may either be internally mounted or deployed on booms [Ref. 3:p. 250]. The magnetometers consist of a coil around a ferromagnetic core of known permeability and area. When in the presence of a magnetic field, a voltage is produced that is proportional to the field component along the solenoid axis and is given by

$$V = -AN \mu (dB_i/dt) \quad (2.4)$$

where B_i is the field component [Ref. 3:p. 181]. By combining the field components from the three magnetometers, the solenoid axis directions can be computed. If the

solenoid axes are aligned with the body axes, the attitude angles can easily be found.

Errors in the magnetometers may be the result of the model used to predict the earth's magnetic field, the influence of the satellite's electrical components, crosstalk between the magnetometers or a misalignment of the solenoid axis. At high orbital heights, the exact magnitude and direction of the earth's magnetic field is not well known and the model used to predict the magnitude and direction of the flux lines may include considerable errors. At altitudes above 1000 km, the field strength decreases as the inverse cube of the distance and the magnetic field of the satellite may dominate. Crosstalk involves the influence of one magnetometer on the others as a result of eddy currents that are produced. Misalignment may occur if the solenoid axis is not aligned with the body axis. This may occur upon deployment or if there is some deformation of the boom during a spinning maneuver. [Ref. 3:pp. 181,182,250]

D. NUTATION

All sensor measurements described so far have assumed that the satellite was not nutating. If nutation occurs, the sensor data will exhibit an oscillatory behavior. The frequency of oscillation is the same as the body nutation rate ω_n . This motion can be used to calculate the nutation

angle directly from sensor data. The derivation and details are given on pages 539-548 of Reference 5.

If the nutation is monitored by a sun sensor, then the maximum nutation angle is given by

$$\eta = \delta\beta / 2R_{\beta} \quad (2.6)$$

where $\delta\beta$ is the range of nominal sun vectors and R_{β} is the ratio of observed sun angle variations to the maximum nutation amplitude. R_{β} is dependent on the satellite's moments of inertia and the location of the sun sensor [Ref. 3:p. 250].

Knowing the nutation angle and the attitude angles, the satellite can determine when to fire control thrusters to reduce nutation and reorient itself. This can either be done autonomously or via the telemetry link. Examples of active nutation control and orientation are given in Chapter V.

III. ATTITUDE DYNAMICS AND CONTROL

A. ATTITUDE DYNAMICS

Newton and Euler first described the motion of a system of particles in inertial and rotational frames of reference. These are described and detailed in a number of publications. This chapter will present a summary of these derivations as they relate to modelling ORION's motion.

The satellite operates with respect to a reference frame which rotates around the earth in the orbital plane. As was shown in Figure 1.3, the x axis is in the direction of flight, the z axis points towards the earth and the y axis is perpendicular to the orbital plane.

The orbital axes are related to the fixed reference frame of the earth by the direction cosine matrix \bar{C} . \bar{C} is a linear combination of Euler rotations defined as

$$\bar{C} = F_b \cdot F_i$$

where F_b is the body reference frame and F_i is the inertial reference frame [Ref. 5:p. 23]. The three rotations are

$$C(\phi) = \begin{bmatrix} 1 & 0 & 0 \\ 0 & \cos \phi & \sin \phi \\ 0 & -\sin \phi & \cos \phi \end{bmatrix} \quad (3.1)$$

$$C(\Theta) = \begin{bmatrix} \cos \Theta & 0 & -\sin \Theta \\ 0 & 1 & 0 \\ \sin \Theta & 0 & \cos \Theta \end{bmatrix} \quad (3.2)$$

$$C(\Psi) = \begin{bmatrix} \cos \Psi & \sin \Psi & 0 \\ -\sin \Psi & \cos \Psi & 0 \\ 0 & 0 & 1 \end{bmatrix} \quad (3.3)$$

The most commonly used sequence is the 3-2-1 sequence which results in

$$C = \begin{bmatrix} \cos \Psi \cos \Theta & \sin \Psi \cos \phi & \sin \Psi \sin \phi \\ -\sin \Psi \cos \Theta & \cos \Psi \cos \phi & \cos \Psi \sin \phi \\ -\sin \Theta & -\sin \phi \cos \Theta & \cos \Theta \cos \phi \end{bmatrix} \quad (3.4)$$

The satellite orientation is related to the orbital axes by the body fixed coordinate axes (x,y,z). The deviations of the body axes and the orbital axes are given by the angles ϕ (phi), Ψ (psi), and Θ (theta).

There are six Euler equations that govern satellite motion [Ref. 5:p. 32]. They are:

$$\dot{\mathbf{p}} = \boldsymbol{\omega} * \mathbf{p} + \mathbf{f} \quad (3.5)$$

$$\mathbf{p} = m\mathbf{v} \quad (3.6)$$

$$\dot{\mathbf{R}}_C = \mathbf{v} \quad (3.7)$$

$$\dot{\mathbf{h}} = -\boldsymbol{\omega} * \mathbf{h}_C + \mathbf{T} \quad (3.8)$$

$$\mathbf{h} = \mathbf{I}\boldsymbol{\omega} \quad (3.9)$$

$$\dot{\mathbf{C}} = -\boldsymbol{\omega} * \mathbf{C} \quad (3.10)$$

where ω^* is defined as

$$\omega^* = \begin{bmatrix} 0 & -\omega_z & \omega_y \\ \omega_z & 0 & -\omega_x \\ -\omega_y & \omega_x & 0 \end{bmatrix} \quad (3.11)$$

Equations (3.5), (3.6), and (3.7) are the translation equations of motion and are not discussed in this thesis. Equations (3.8), (3.9), and (3.10) apply to the attitude control of ORION.

The moment of inertia about an axis is the sum of the masses times the square of the distance of the mass from the axis. The moment of inertia matrix I is given as

$$I = \begin{bmatrix} I_x & I_{xy} & I_{xz} \\ I_{yx} & I_y & I_{yz} \\ I_{zx} & I_{yz} & I_z \end{bmatrix} \quad (3.12)$$

where $I_x = \int x^2 dm$, $I_y = \int y^2 dm$, $I_z = \int z^2 dm$. Since ORION is a symmetrical body with the body axes centered at the center of mass, the cross-products of inertia, I_{xy} , I_{yz} and I_{zx} are zero.

Expanding Equation (3.8) into x , y , and z components yields

$$\dot{h}_x = \omega_z h_y - \omega_y h_z + T_x \quad (3.13)$$

$$\dot{h}_y = \omega_x h_z - \omega_z h_x + T_y \quad (3.14)$$

$$\dot{h}_z = \omega_y h_x - \omega_x h_y + T_z \quad (3.15)$$

Expanding Equation (3.9) and substituting into (3.13), (3.14), and (3.15) and solving for T yields

$$T_x = I_x \dot{\omega}_x + (I_z - I_y) \omega_y \omega_z \quad (3.16)$$

$$T_y = I_y \dot{\omega}_y + (I_x - I_z) \omega_x \omega_z \quad (3.17)$$

$$T_z = I_z \dot{\omega}_z + (I_y - I_x) \omega_y \omega_x \quad (3.18)$$

T_i is the sum of the external torques on the satellite in the i th axis. These torques include environmental torques, control torques and any other torques which may affect the satellite. Torques will be discussed later in the chapter.

Since ORION is symmetric about the x and z axes, $I_x = I_z = I_t$, the transverse moment of inertia. The y axis is also the spin axis and $I_y = I_a$. The angular velocity vector $\bar{\omega}$ decomposes into its Euler angle components: [Ref. 4:p. 30]

$$\omega_x = \dot{\phi} - \psi \omega_0 \quad (3.19)$$

$$\omega_y = \dot{\theta} - \omega_0 \quad (3.20)$$

$$\omega_z = \dot{\psi} + \phi \omega_0 \quad (3.21)$$

ORION will spin such that the spin axis is in the negative y direction. This means that

$$\omega_y = \omega_0 - \dot{\theta} \quad (3.22)$$

In the absence of external torques the motion equations reduce to

$$I_t \dot{\omega}_x = (I_a - I_t) \omega_y \omega_z \quad (3.23)$$

$$I_t \dot{\omega}_y = 0 \quad (3.24)$$

$$I_t \dot{\omega}_z = (I_t - I_a) \omega_y \omega_x \quad (3.25)$$

Equation (3.24) implies that ω_y is a constant. Differentiating Equations (3.23) and (3.25) and substituting for $\dot{\omega}_x$ and $\dot{\omega}_y$ yields

$$\ddot{\omega}_x + \frac{(I_a - I_t)(I_a - I_t)}{I_t^2} \omega_y^2 \omega_x = 0 \quad (3.26)$$

$$\ddot{\omega}_z + \frac{(I_a - I_t)(I_a - I_t)}{I_t^2} \omega_y^2 \omega_z = 0 \quad (3.27)$$

For stability, the coefficients of ω_x and ω_z must be positive. The y axis is the maximum moment of inertia when $I_a > I_t$ and is the minimum moment of inertia when $I_t > I_a$. If there is no energy dissipation, the satellite is stable if spun about either the maximum or minimum moment of inertia. If there are external torques or energy dissipation means, the satellite is stable only if spun about the maximum moment of inertia [Ref. 4:p. 112].

Since there are external torques present, these must be taken into account when calculating the attitude of the satellite. Substituting for ω in Equations (3.16), (3.17), and (3.18),

$$\begin{aligned} T_x &= I_t (\ddot{\phi} - \omega_o \dot{\psi}) + (I_t - I_a) (\omega_o - \dot{\theta}) (\dot{\psi} + \omega_o \phi) \\ &= I_t \ddot{\phi} - I_t \omega_o \dot{\psi} + (I_t - I_a) (\omega_o \dot{\psi} + \omega_o^2 \phi - \dot{\theta} \dot{\psi} - \omega_o \dot{\theta} \phi) \\ &= I_t \ddot{\phi} + (I_t - I_a) (\omega_o^2 - \dot{\omega}_o \dot{\theta}) \phi + ((I_t - I_a) (\omega_o - \dot{\theta}) - I_t \omega_o) \dot{\psi} \end{aligned} \quad (3.28)$$

$$T_y = -I_y \ddot{\theta} \quad (3.29)$$

$$\begin{aligned} T_z &= I_t(\ddot{\psi} + \omega_o \dot{\phi}) + (I_a - I_t)(\omega_o - \dot{\theta})(\dot{\phi} - \omega_o \psi) \\ &= I_t \ddot{\psi} + I_t \omega_o \dot{\phi} + (I_a - I_t)(\omega_o \dot{\phi} - \omega_o^2 \psi - \dot{\theta} \dot{\phi} + \omega_o \dot{\theta} \psi) \\ &= I_t \ddot{\psi} + (I_a - I_t)(\omega_o \dot{\theta} - \omega_o^2) \psi + ((I_a - I_t)(\omega_o - \dot{\theta}) + I_t \omega_o) \dot{\phi} \\ &= I_t \ddot{\psi} + (I_t - I_a)(\omega_o^2 - \omega_o \dot{\theta}) \psi - ((I_t - I_a)(\omega_o - \dot{\theta}) - I_t \omega_o) \dot{\phi} \end{aligned} \quad (3.30)$$

Solving for the second derivatives of the Euler angles yields

$$\ddot{\phi} = (T_x - (I_t - I_a)(\omega_o^2 - \omega_o \dot{\theta})\phi - ((I_t - I_a)(\omega_o - \dot{\theta}) - I_t \omega_o)\dot{\psi})/I_t \quad (3.31)$$

$$\ddot{\psi} = (T_z - (I_t - I_a)(\omega_o^2 - \omega_o \dot{\theta})\psi + ((I_t - I_a)(\omega_o - \dot{\theta}) - I_t \omega_o)\dot{\phi})/I_t \quad (3.32)$$

$$\ddot{\theta} = -T_y/I_a \quad (3.33)$$

If ω_o and $\dot{\theta}$ are assumed to be constant the equations can be written

$$\ddot{\phi} = T_x - A\phi - B\dot{\psi} \quad (3.34)$$

$$\ddot{\psi} = T_z - A\psi + B\dot{\phi} \quad (3.35)$$

$$\ddot{\theta} = -T_y/I_a \quad (3.36)$$

where:

$$A = (1 - I_a/I_t)(\omega_o - \dot{\theta})\omega_o$$

$$B = (1 - I_a/I_t)(\omega_o - \dot{\theta}) - \omega_o$$

The block diagram form of the equations is given in Figure 3.1. As can be seen from Figure 3.1, ϕ and ψ are cross-coupled through their rotation rates.

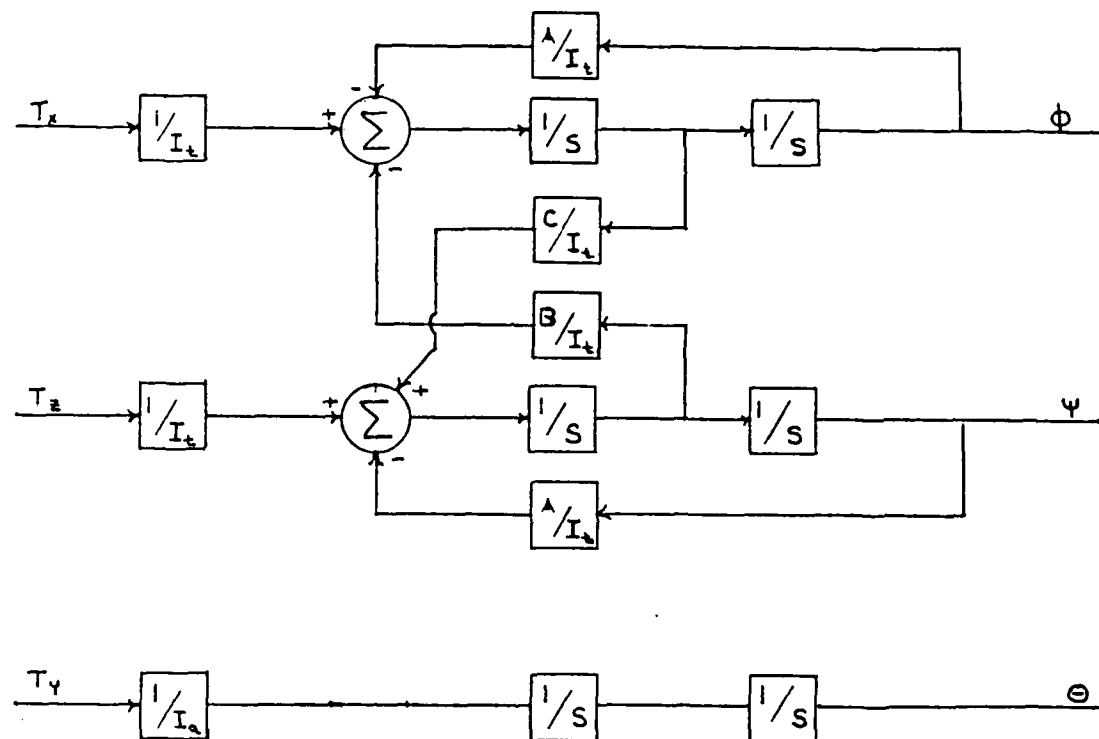


Figure 3.1 System Block Diagram

The total angular momentum vector \bar{H} can be expressed as

$$\bar{H} = I_a \bar{\omega}_y + I_t \bar{\omega}_t \quad (3.37)$$

where $\omega_t^2 = \omega_x^2 + \omega_z^2$ and lies in the x-z plane. ω_t rotates relative to the satellite with the angular velocity λ where

$$\lambda = (I_a/I_t - 1)\omega_y \quad (3.38)$$

The body nutation frequency is defined as

$$\omega_n = I_a/I_t \omega_y \quad (3.39)$$

The motion of the satellite consists of the satellite rotating about its spin axis and the spin axis rotating about \bar{H} with the angular velocity ω_n [Ref. 4:p. 115]. The nutation angle η is defined as

$$\eta = \sin^{-1} \left(\frac{I_t \omega_t}{H} \right) \quad (3.40)$$

Figure 3.2 shows the relationship between ω_t , ω_n , ω_y and \bar{H} .

The inherent stability of the satellite can be found by analyzing the transfer functions of the satellite. Setting T_x and T_z equal to zero and dividing by I_t yields

$$\ddot{\phi} + (1 - I_a/I_t)(\omega_o - \dot{\theta})\omega_o \dot{\phi} + ((1 - I_a/I_t)(\omega_o - \dot{\theta}) - \omega_o)\dot{\psi} = 0 \quad (3.41)$$

$$\ddot{\psi} + (1 - I_a/I_t)(\omega_o - \dot{\theta})\omega_o \dot{\psi} - ((1 - I_a/I_t)(\omega_o - \dot{\theta}) - \omega_o)\dot{\phi} = 0 \quad (3.42)$$

Noting that $-\lambda = (1 - I_a/I_t)(\omega_o - \dot{\theta})$ and taking the Laplace transforms of the equations yields

$$\phi(s)s^2 - \lambda \omega_o \phi(s) - (\lambda + \omega_o)s\psi(s) = 0 \quad (3.43)$$

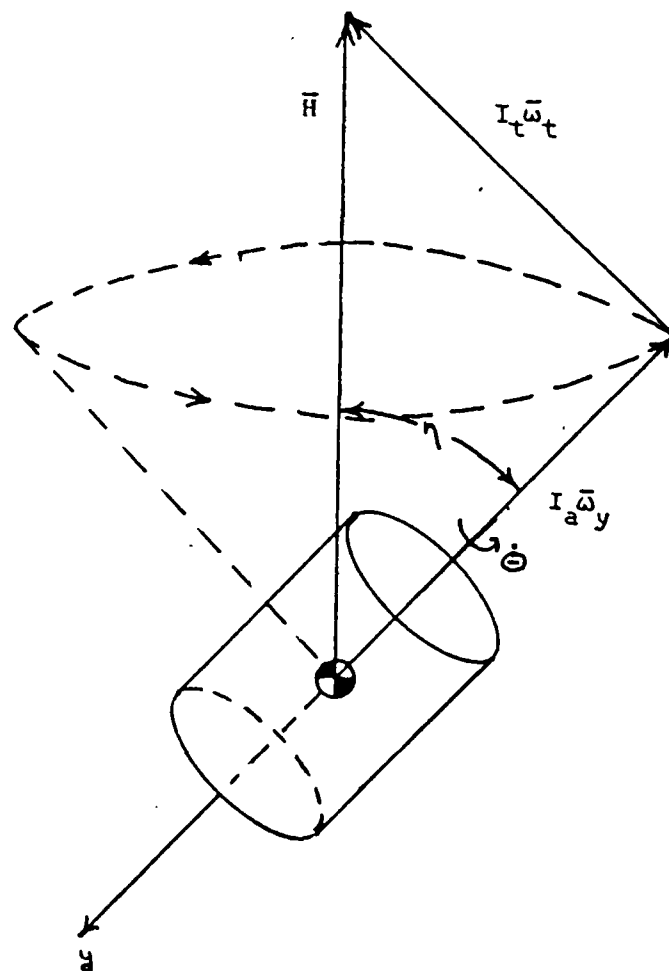


Figure 3.2 Nutation Cone

$$\Psi(s)s^2 - \lambda\omega_0\Psi(s) + (\lambda+\omega_0)s\phi(s) = 0 \quad (3.44)$$

Solving for $\Psi(s)$ and substituting

$$\phi(s)(s^2 - \lambda\omega_0) - \frac{(\lambda+\omega_0)^2 s^2}{(s^2 - \lambda\omega_0)} \phi(s) = 0 \quad (3.45)$$

$$\phi(s)(s^2 - \lambda\omega_0)^2 + (\lambda+\omega_0)^2 s^2 \phi(s) = 0 \quad (3.46)$$

$$\phi(s)(s^4 + (\lambda+\omega_0)^2 - \lambda\omega_0)s^2 + \lambda^2\omega_0 = 0 \quad (3.47)$$

Partitioning

$$\phi(s) = 1 + \frac{\lambda^2\omega_0^2}{s^2(s^2 + ((\lambda+\omega_0)^2 - \lambda\omega_0))} \quad (3.48)$$

The open loop transfer function is

$$\frac{\lambda^2\omega_0^2}{s^2(s^2 + ((\lambda+\omega_0)^2 - \lambda\omega_0))} \quad (3.49)$$

The transfer function has two poles at the origin and two poles on the imaginary axis at $+j\sqrt{(\lambda+\omega_0)^2 - \lambda\omega_0}$ and $-j\sqrt{(\lambda+\omega_0)^2 - \lambda\omega_0}$. Therefore, the stability of the satellite depends on spin rate, inertia ratio and orbit altitude. Table 3.1 shows the root locations for different σ and ω_y .

Because there is no cubed term in the transfer function, the roots will always be on the imaginary axis. This implies that the satellite will tend to reach a new steady-state value for ϕ and Ψ if perturbed, rather than return to an initial state.

TABLE 3.1
ROOTS OF THE TRANSFER FUNCTION
($\omega_0 = .001184$)

γ	σ	λ	Root Location on Imaginary Axis
-6.283	0.3635	3.999	4.00
	1.4882	-3.067	3.066
-2.094	0.3635	1.333	1.334
	1.4882	-1.022	1.022
-1.047	0.3635	.6664	.667
	1.4882	- .5111	.5106

B. ENVIRONMENTAL TORQUES

Before the motion of ORION can be accurately modelled, the possible external disturbances must be studied. The major disturbances experienced by a satellite in low earth orbit are aerodynamic drag and gravity gradient torques.

Aerodynamic drag is a result of the motion of the satellite through the upper atmosphere. It can be expressed as

$$D = \frac{1}{2} \rho V^2 C_D A \quad (3.50)$$

where:

- ρ = density of air at orbit altitude
- V = velocity of satellite along orbit
- C_D = drag coefficient
- A = surface area over which the drag acts.

The drag on the body can be represented by a single force acting on the body's center of pressure. If this center of pressure is located away from the center of mass, a torque is developed.

The velocity of the satellite is

$$V = \omega_o R \quad (3.51)$$

$$\omega_o^2 = \mu_e / R^3 \quad (3.52)$$

$$V^2 = \mu_e / R^3 \cdot R^2 = \mu_e / R \quad (3.53)$$

where:

μ_e = gravitational constant

R = distance of satellite from earth's center.

The density of air decreases as the altitude increases. At a 200 km orbit the air density is approximately 7.0×10^{-10} kg/m³. The surface area is the cross-sectional area of the satellite; for ORION, $A = 0.429$ m². Drag coefficients vary with shape, material smoothness, etc. A typical value for this type of satellite is $C_D = 2$. The drag can be expressed as

$$D = \frac{1.71 \times 10^{14}}{R} \quad (3.54)$$

The center of pressure for ORION is assumed to be located 0.076 m along the positive y axis. Since the drag acts opposite to the direction of flight, the total drag torque on ORION can be expressed as

$$T_D = D * L * \cos \psi \quad (3.55)$$

where L is 0.076 m.

The second major disturbance is due to the gravity gradient that exists as the distance from the earth increases. The gravity gradient torque is defined as

$$G = \frac{3\mu_e}{R_o^5} \int (r \times R) (r \cdot R) \, dm \quad (3.56)$$

where:

R = position vector of the satellite with respect to the earth; and

r = coordinate of an elemental mass from the center of mass. [Ref. 4:p. 131]

Using the 3-2-1 Euler rotation between the body axes and the orbit fixed axis, the gravity gradient torques are

$$G_x = 3\omega_o^2 [(I_t - I_a) \sin \phi \cos \phi \cos^2 \theta] \quad (3.57)$$

$$G_y = 0 \quad (3.58)$$

$$G_z = 3\omega_o^2 [(I_t - I_a) \sin \theta \cos \theta \sin \phi] \quad (3.59)$$

Thus gravity gradient torques depend on orbital altitude, moments of inertia and satellite orientation.

The equations describing aerodynamic drag and gravity gradient torques can now be used in simulating their effect on satellite motion. The analysis of this effect is contained in Chapter IV.

C. COMPUTER MODELS

The computer model was written in the Dynamic Simulation Language (DSL). The program listing is contained in the Appendix. The program was intended to be as general as possible to allow it to apply to a variety of parameter changes. Of special interest are I_t , I_a , orbital altitude, air density, and spin rate.

The three Euler equations are integrated once to obtain $\dot{\phi}$, $\dot{\theta}$ and $\dot{\psi}$. These are integrated again to obtain ϕ , θ , and ψ . The initial values depend on the situation being analyzed. Once the attitude angles have been calculated, they can be used to calculate ω_t , ω_n , λ and the nutation angle.

Also included is the equation governing magnetometer deployment. It is implemented in the form of a ramp function. The starting time is the time when the magnetometer is to be deployed. The ending time is calculated by dividing the desired boom length by 0.0169. If no boom length change is desired the ramp function can be commented out of the program and the variable L_b set to the desired boom length. An L_y of zero indicates that the magnetometers are in the storage position.

Changes in spin rates can be accomplished in two ways. One is to change the initial condition of $\dot{\psi}$ in a PARAM statement. This is useful when evaluating the effect of configuration changes at different spin rates. The second

method simulates the use of the spin-up thrusters. T_y can be a step, ramp, or pulse input, or any combination that approximates the actual thruster firing profile.

In addition to the variables describing moments of inertia, spin rate, and thruster torque, many other components of the model are left as variable quantities in the program. These can be changed by PARAM statements in multiple runs to provide the widest range of possible parameter studies.

IV. PARAMETER STUDIES AND ACQUISITION SIMULATION

A. SIMULATION MODEL

The design of any modern system involves the investigation and analysis of how the system responds to inputs with a given set of system parameters. These parameter studies are used in design and cost trade-offs which will eventually lead to the optimum system design. One way to run parameter studies is to use scale models and testing chambers. These are primarily used in the final design stages. In preliminary design where there are a lot of variables computer simulations are best performed.

The computer model described in Chapter III was used to analyze some parameter changes that may be associated with ORION. It is expected that this model will be used to determine the optimum configuration in terms of moments and magnetometer deployment. This chapter analyzes the changes in inertia ratio and spin rates as a result of a typical mission. It also analyzes the environmental effects of gravity gradient and aerodynamic drag.

B. PARAMETER STUDIES

The first study was to analyze how a change in the moments of inertia would affect the spin rate and stability. The current mission requires the deployment of four 0.907 kg (2 lb) magnetometers on lightweight booms. The booms were

assumed to deploy at a constant rate of 0.0169 m/sec to a maximum of 3.048 m (10 ft). The mass of the booms was considered to be negligible and did not contribute to the inertia of the satellite. The magnetometers are located in the x-z plane of the satellite as shown in Figure 4.1.

The effect of deploying the magnetometers is to increase both I_a and I_t . The new moments of inertia can be calculated by finding the moment of inertia for the satellite without the magnetometers and then adding the moment of inertia for each magnetometer. Thus

$$I_a = 0.5m_s r^2 + 4m_m(l_b + r)^2 \quad (4.1)$$

$$I_t = 0.083m_s(3r^2 + h^2) + 2m_m(l_b + r)^2 \quad (4.2)$$

where:

m_s = mass of satellite minus the mass of 4 magnetometers

m_m = mass of one magnetometer

r = radius of the satellite

h = height of the satellite

l_b = distance of the magnetometer from the outside of the satellite.

Substituting in the values for ORION, the moments of inertia can be found at any boom length by

$$I_a = 3.203 + 3.628(l_b + 0.242)^2 \quad (4.3)$$

$$I_t = 8.81 + 1.81(l_b + 0.242)^2 \quad (4.4)$$

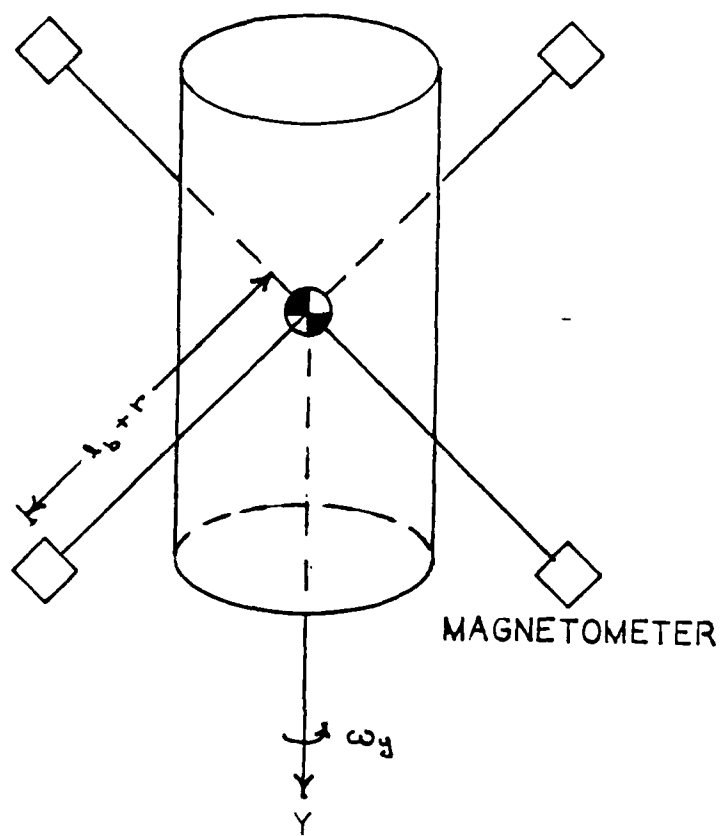


Figure 4.1 Magnetometer Deployment Diagram

Figure 4.2 shows this relationship between the boom length and the moments of inertia. I_a becomes larger than I_t at a boom length of 1.53 m. If energy could be dissipated, then with I_a larger than I_t the satellite would become stable about the spin axis [Ref. 4:p. 117].

Deployment of magnetometers also has an effect on the spin rate and could be used to change it without using the spin-up thrusters. Using the principle of the conservation of angular momentum, if ω_t is assumed to be zero then

$$H = I_a \omega_y \quad (4.5)$$

and as I_a increases ω_y must decrease. Figure 4.3 shows how the spin rate changes with boom length.

As noted earlier, the magnetometer deployment can be used to change the spin rate of the satellite. If the satellite is spinning at 60 rpm ($\omega_y = -6.283$ rad/sec), a boom length of 1.097 m will slow the spin to 20 rpm ($\omega_y = -2.094$ rad/sec). A 1.87 m deployment will slow the spin to 10 rpm ($\omega_y = -1.047$ rad/sec). Adjusting the boom length to reach a specific spin rate is applicable if the mission does not require the magnetometers a specific distance from the satellite. It is more probable that the boom must be a specific length and the satellite must spin at a specific rate.

There are two ways to achieve this configuration. The first method is to deploy the magnetometer to the desired length, then adjust the spin as necessary with the

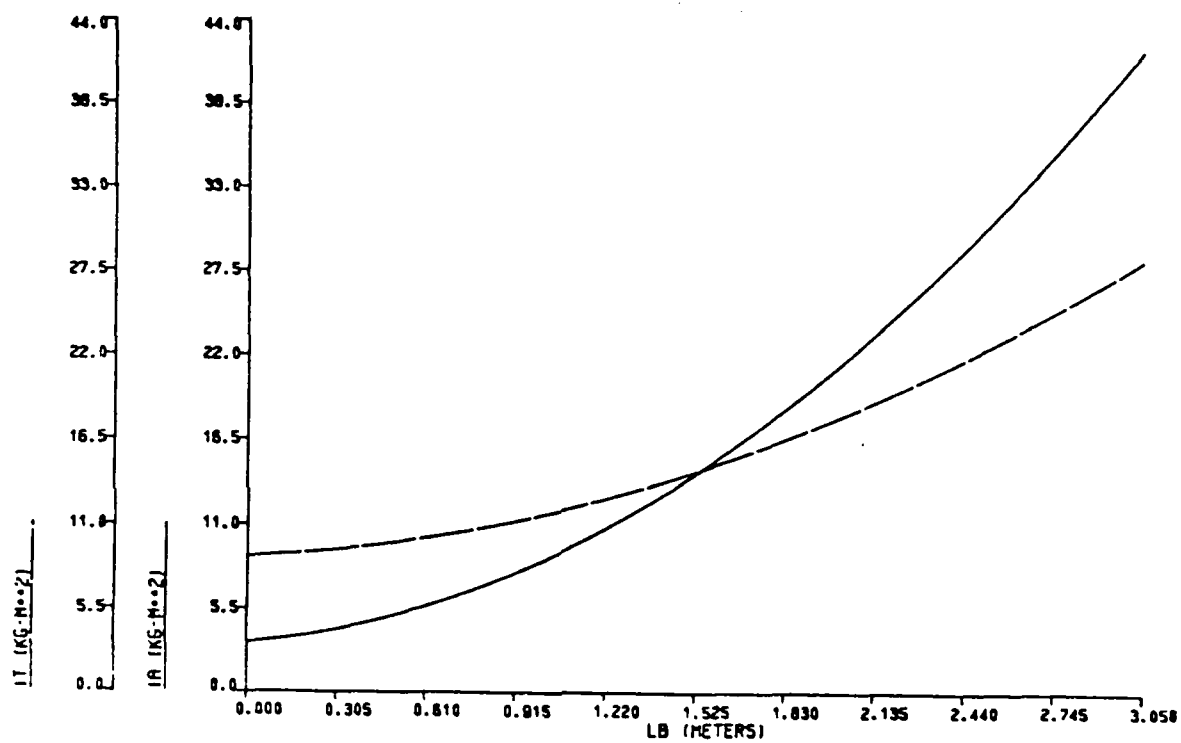


Figure 4.2 Change in Moments of Inertia with Boom Length

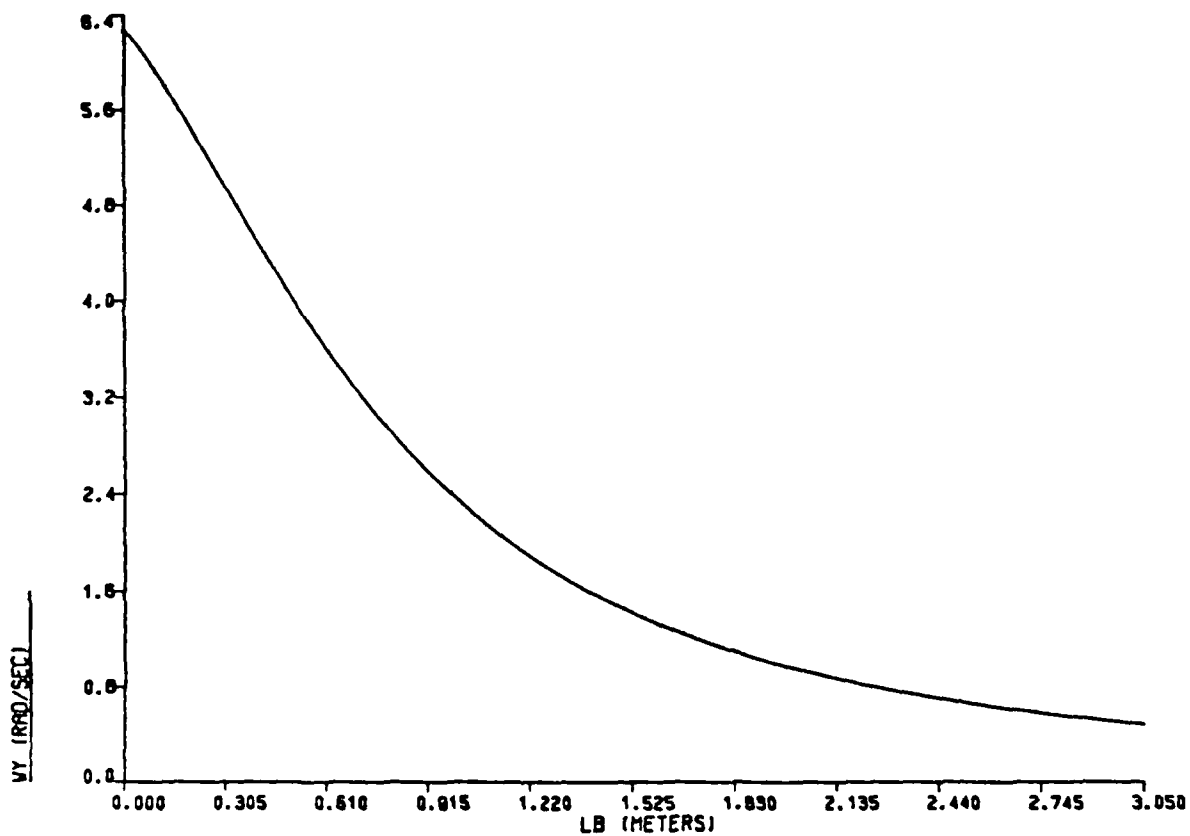


Figure 4.3 Change in Spin Rate with Magnetometer Deployment

thrusters. A second method is to despin the satellite with the thrusters then deploy the magnetometers and readjust the spin with the thrusters. If the change in spin and boom length is small, it may be possible to despin the satellite to a rate such that the subsequent deployment of the booms will despin the satellite to the required rate.

Since the firing interval of the thrusters is proportional to the amount of fuel used, it can be used to compare the two methods. To illustrate this, assume the satellite is initially spinning at 60 rpm with $I_a = 3.239$ kg-m². A boom length of 2 m and a spin rate of 20 rpm is required. At 2 m, I_a is 21.447 kg-m². Using the first method, after deployment the spin rate is

$$\begin{aligned}\omega_{y2} &= \frac{I_{a1}\omega_{y1}}{I_{a2}} \\ &= \frac{(3.239)(-6.283)}{21.477} \\ &= -0.9476 \text{ rad/sec} \quad (4.6)\end{aligned}$$

Assuming the total torque of the thrusters is $F \times R = 0.2168$ n-m, the firing interval dt is

$$\begin{aligned}dt &= \frac{I_{a2}(2.094 - \omega_{y2})}{F \times R} \\ &= \frac{(21.447)(2.094 - 0.9476)}{0.2168} \\ &= 113.3 \text{ sec} \quad (4.7)\end{aligned}$$

Using the second method, the firing interval required to despin the satellite to 20 rpm is

$$\begin{aligned} dt &= \frac{(3.239)(6.283-2.093)}{(0.2168)} \\ &= 62.6 \text{ sec} \end{aligned} \quad (4.8)$$

Deploying the magnetometer to 2 meters causes the spin rate to decrease to 0.3152 rad/sec. The firing interval required to readjust the spin is 176.1 sec. The total firing interval for the second method is 238.7 sec, more than twice that of the first method.

This indicates that the first method is more fuel efficient in deploying the magnetometers and achieving a specific spin rate. A disadvantage of both these methods is that if the booms are too flexible, adjusting the spin may cause the magnetometers to lag the boom-satellite attachment points and cause too great a stress in the booms.

1. Stability

Whether σ is changed by deploying magnetometers or by changing the internal mass distribution of the satellite, it will have an effect on the stability of the satellite. Figure 4.4 shows how a change in σ affects λ and ω_n . Since the roots of the open loop transfer function depend on λ , they also change with σ as was shown in Table 3.1. Figure 4.5 shows the responses of the satellite to a 1.0 n-m pulse of 0.01 sec as σ changes. This was done at three different spin rates of 60 rpm, 20 rpm, and 10 rpm. The advantage of

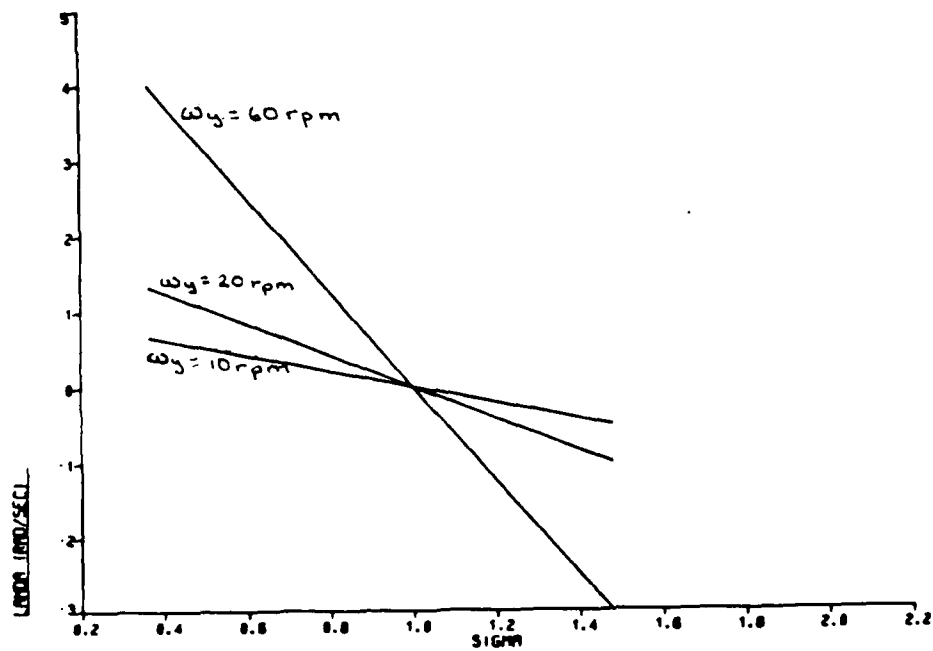
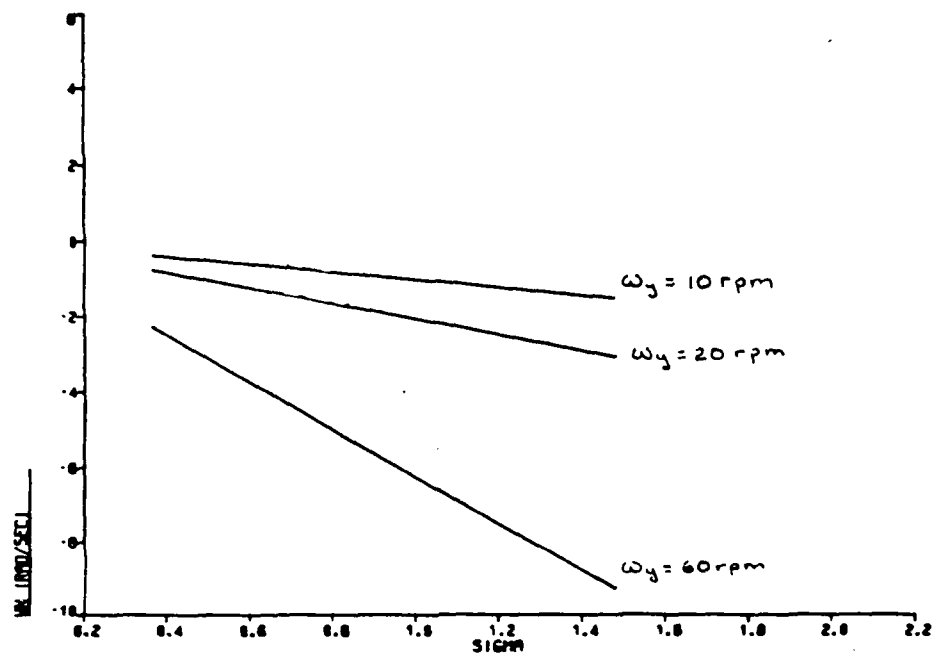


Figure 4.4 The Effects of Inertia Ratio on Nutation Frequencies

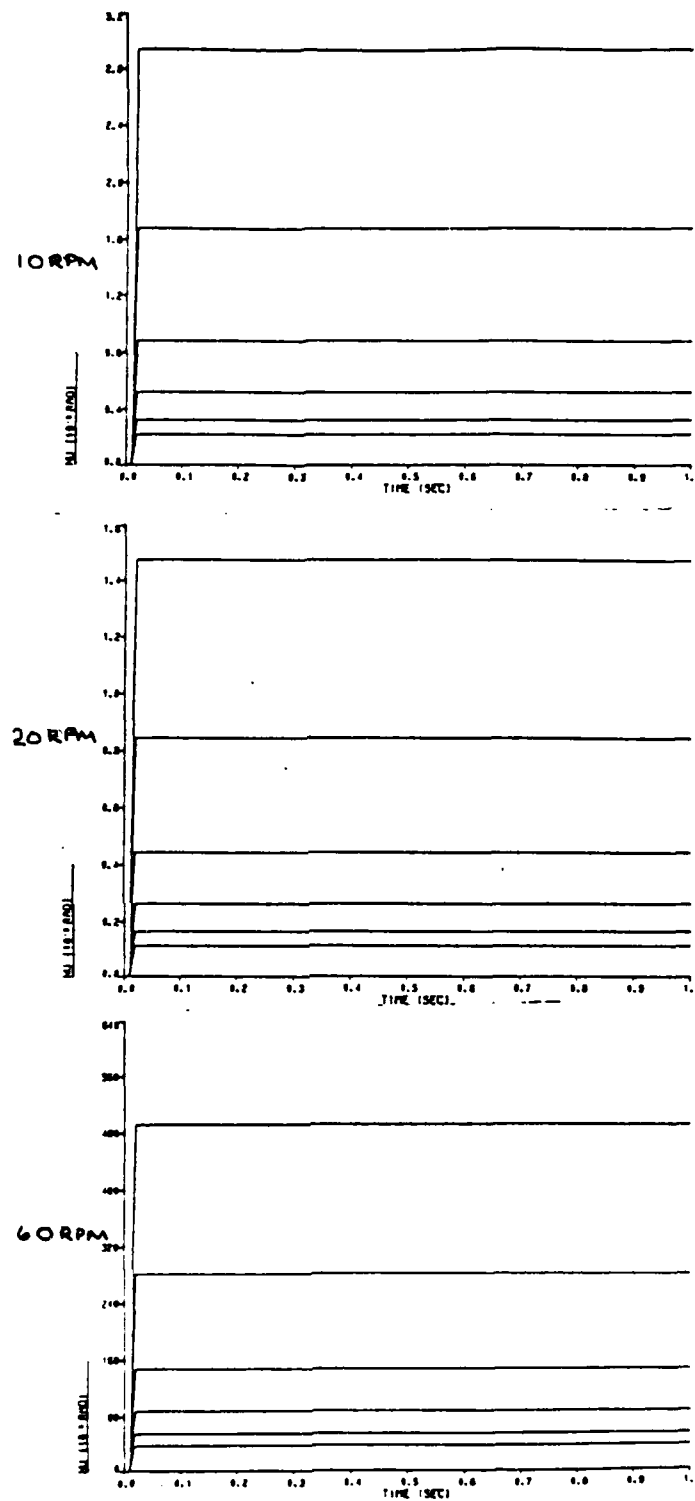


Figure 4.5 Satellite Response to a Short Duration Torque

increasing σ is to make the satellite less susceptible to nutation. Figure 4.6 shows that the higher the spin rate and the larger the inertia ratio, the smaller the nutation will be for a given input torque.

C. ENVIRONMENTAL EFFECTS

The aerodynamic drag and gravity gradient torques were modelled using the equations in Chapter III. These equations were incorporated into the simulation to see what effect they would have on the satellite.

Since the drag force is dependent on the density of the atmosphere, it decreases as the orbit height increases. This is shown in Table 4.1. At an altitude of 200 km the drag torque is 1.383×10^{-3} n-m and decreases to 1.762×10^{-9} at an altitude of 1000 km.

TABLE 4.1
TYPICAL VALUES FOR AERODYNAMIC DRAG

ALT (km)	Density (kg/m ³)	Drag (n)	T _D (n-m)
100	6×10^{-7}	15.84	1.204
200	7×10^{-10}	.0182	1.383×10^{-3}
400	1×10^{-11}	2.523×10^{-4}	1.917×10^{-5}
1000	1×10^{-15}	2.318×10^{-8}	1.762×10^{-9}

Gravity gradient torque is also dependent on orbital altitude since it depends on ω_0 . Unlike drag, however,

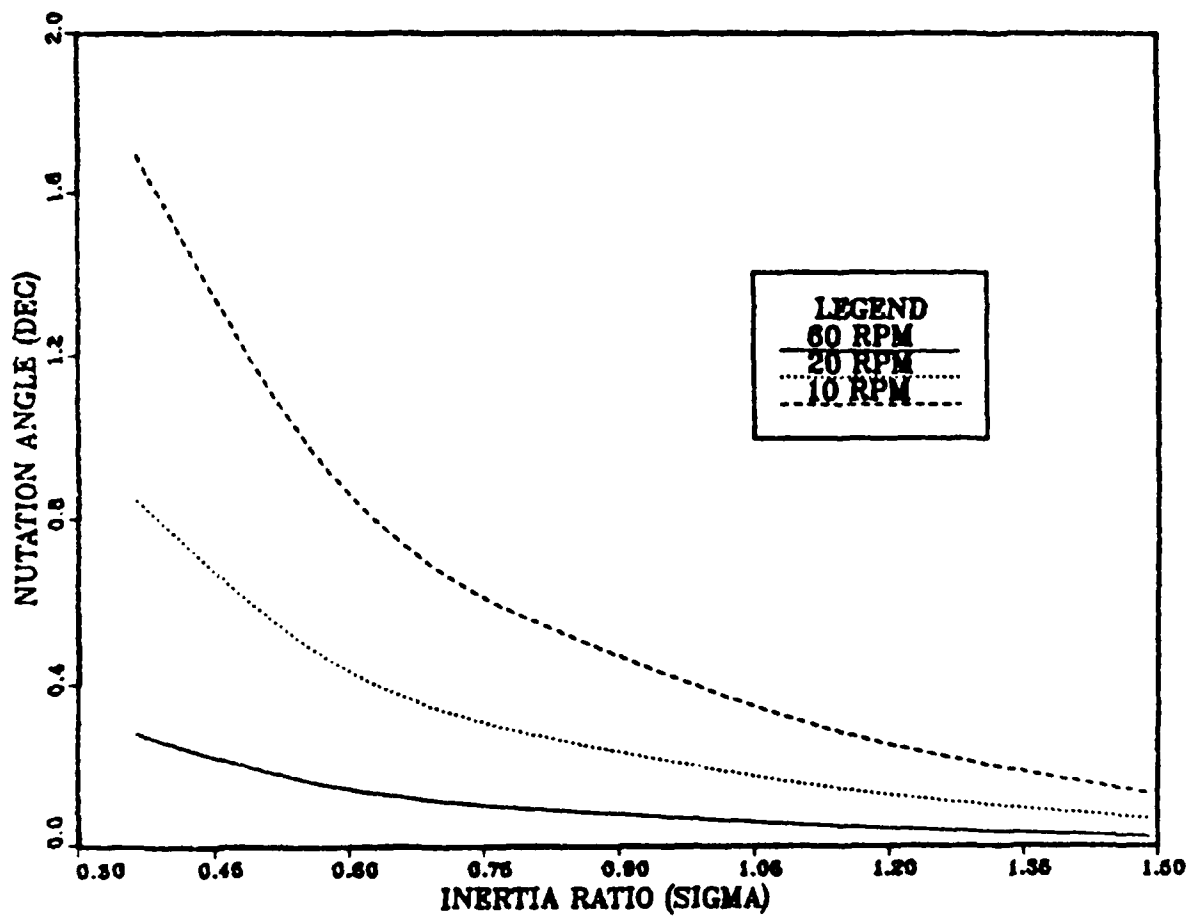


Figure 4.6 Nutation Angles for Different Spins and Inertias

gravity gradient torque is not a constant but depends on the moments of inertia and the orientation of the satellite. At an altitude of 200 km the maximum torque is 3.99×10^{-9} n-m. This decreases to 3.72×10^{-15} n-m at 1000 km.

An orbital altitude of 200 km was used to determine the effect environmental forces have on ORION. Inertia ratios of 0.364 and 1.488 and spin rates of 10, 20 and 60 rpm were used to give the widest ranges of results. These results are shown in Figures 4.7, 4.8 and 4.9. At 10 rpm the maximum nutation is 2.053×10^{-3} radians for a σ of 0.364 and 5.33×10^{-5} radians for a σ of 1.488. At 20 rpm the nutation angles are 5.173×10^{-4} radians and 1.17×10^{-5} radians and for 60 rpm they are 6.0×10^{-5} radians and 1.33×10^{-6} radians.

As can be seen in the figures, the nutation is oscillatory. This is because of the oscillatory nature of the environmental torques, principally the gravity gradient. When the satellite nutates to its maximum angle, the torque effect is reversed causing the nutation to decrease. When the nutation is zero, the torque effect is again reversed and the process repeats itself. The frequency of the effect is related to the spin rate of the satellite. This is seen in the $\dot{\theta}$ term of the torque equations.

If the accuracy requirement of the attitude control system is small enough, environmental effects must be taken into account in the simulations. They will be ignored in

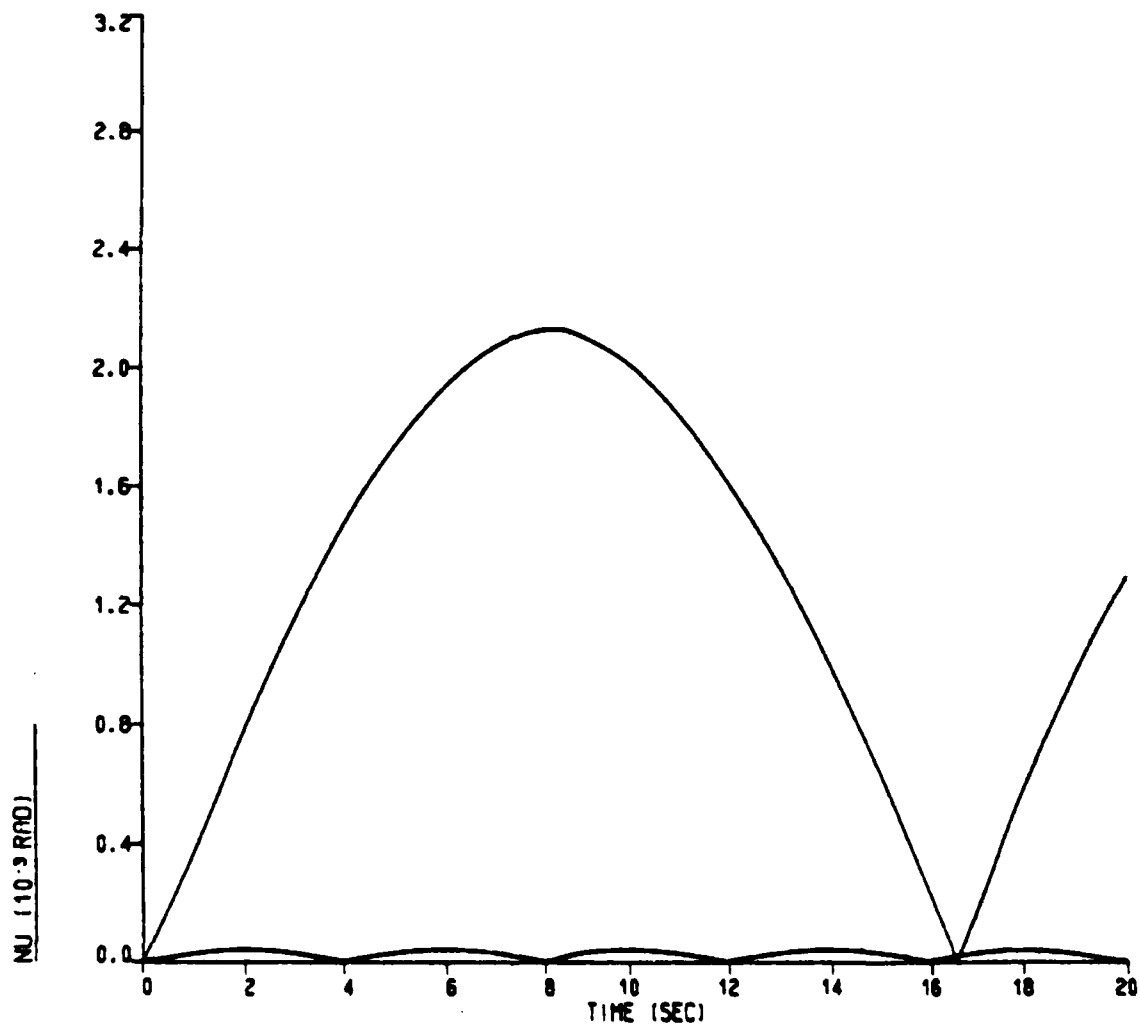


Figure 4.7 Nutation Due to Environmental Torques; 10 Rpm

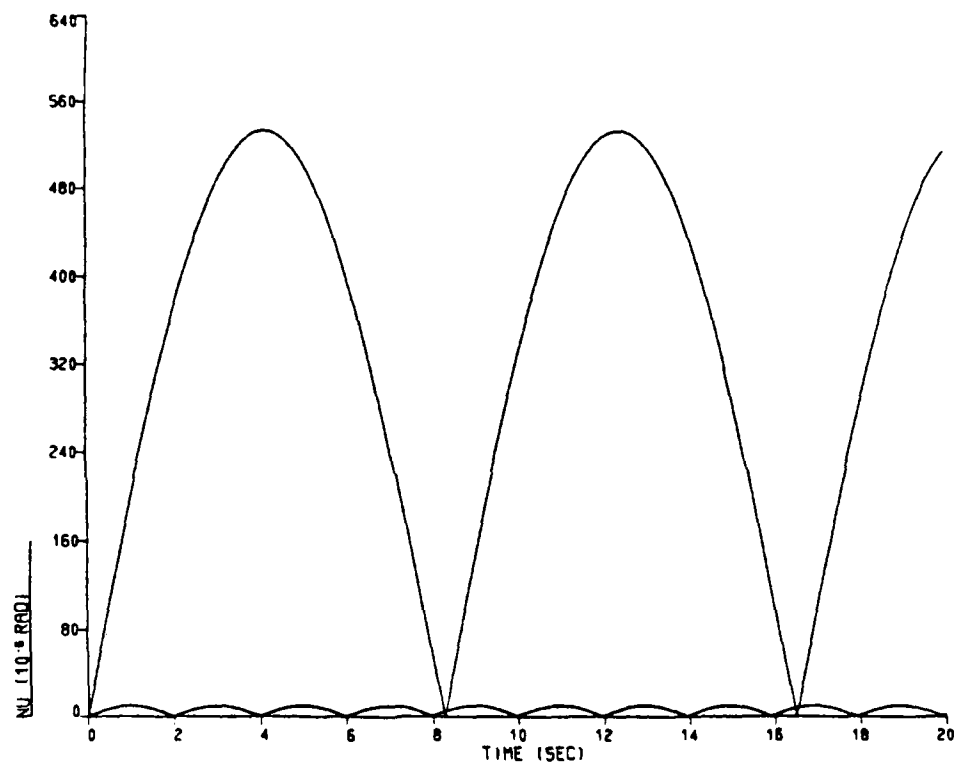


Figure 4.8 Nutation Due to Environmental Torques; 20 Rpm

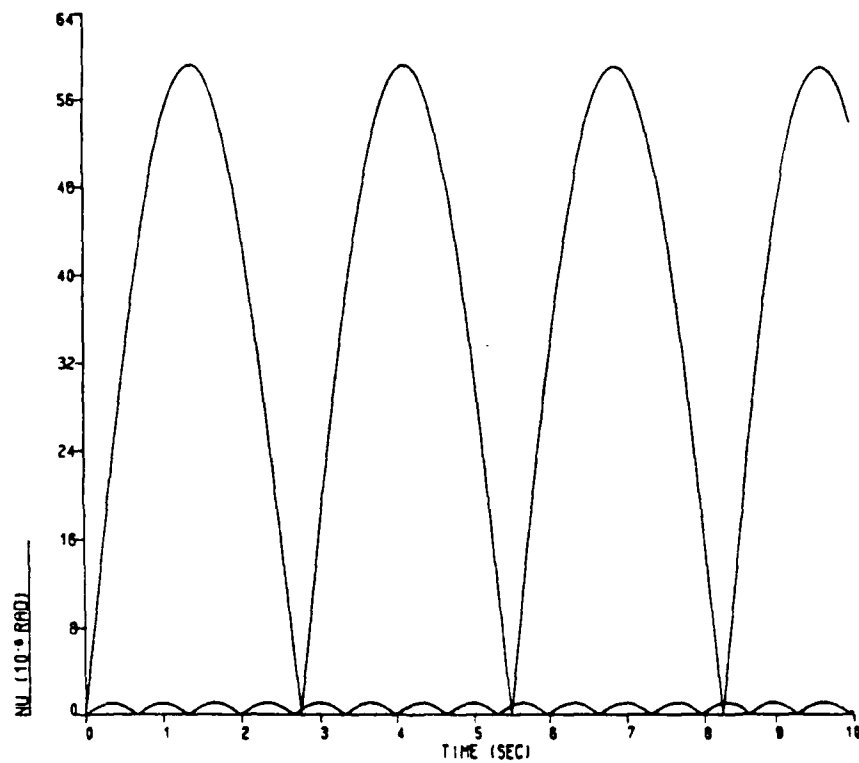


Figure 4.9 Nutation Due to Environmental Torques; 60 Rpm

further simulations described in this thesis since their effect is less than the 2 degree accuracy requirement of ORION. This will simplify the model without a large error in accuracy.

D. ACQUISITION PHASE PROFILE

After analyzing the effects of σ changes and environmental torques, the next step was to simulate the motion of the satellite from launch to spin-up. Drag and gravity gradients effects were included in this simulation.

The flight profile consisted of launching the satellite with no spin. All initial values of ϕ , ψ and θ were assumed to be zero. At 50 seconds a step input of $T_y = 0.2168$ n-m was applied. This caused the value of ω_y to increase. At 144 seconds the input was removed. The value of ω_y was -6.29 rad/sec (60 rpm). Figure 4.10 shows how σ and ψ change during this portion of the mission.

During the drift period environmental torques cause the satellite to rotate 0.013 degrees in roll and 11.04 degrees in yaw. As the spin increases the σ and ψ begin an oscillatory motion. The amplitude of the motion depends on the spin rate. As the spin rate increases, the satellite becomes more resistive to torque effects. When the spin rate becomes a constant, the amplitude of oscillation due to environmental torques becomes a constant although the scale in Figure 4.10 is too large to show this. At 144 seconds, ϕ is 3.89 degrees and ψ is 12.54 degrees. The nutation

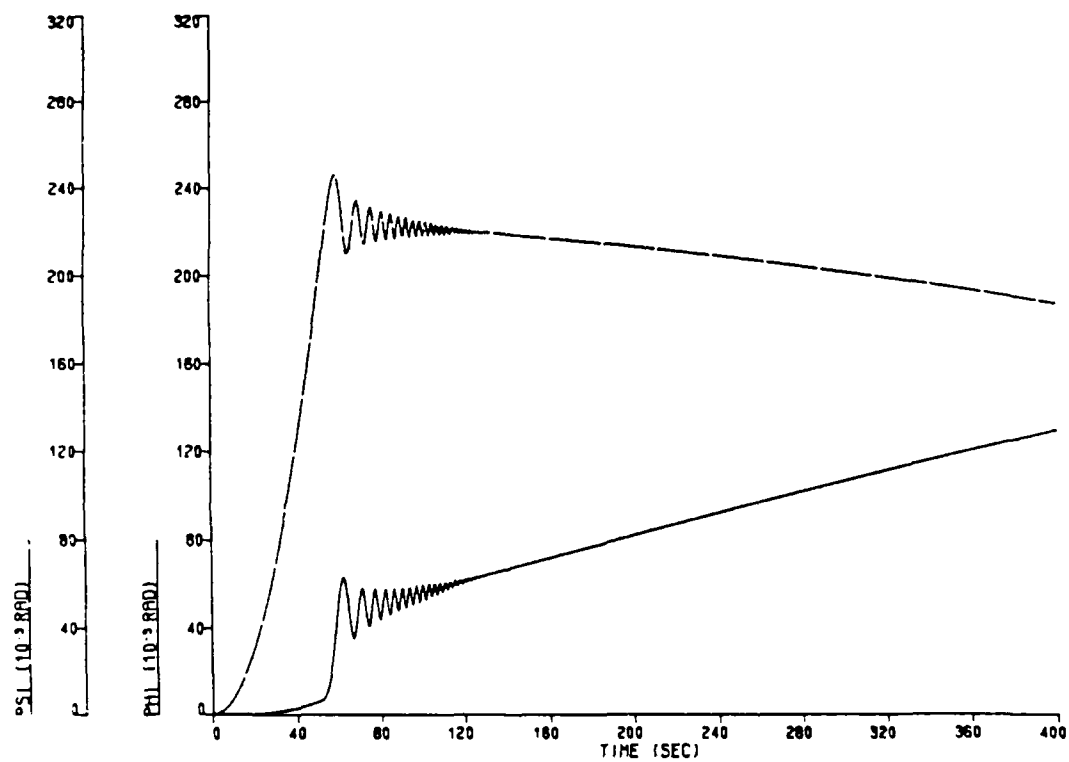


Figure 4.10 Acquisition Phase Roll and Yaw

caused by environmental torques is 0.0015 degrees, much less than the acceptable nutation of 2 degrees. After 400 seconds with no controlling inputs, ϕ is 7.4 degrees, ψ is 10.8 degrees and the nutation is 0.0015 degrees.

From this point, the magnetometers could be deployed or control torques could be applied to reorient the satellite. Chapter V discusses the methods of controlling nutation and reorienting the satellite.

V. MISSION PHASE SIMULATION

A. SATELLITE CONTROL

The process of maintaining the correct orientation of a satellite consists of eliminating the precession and nutation effects caused by external or internal disturbances. The simplest case is when the spin axis and angular momentum vector are aligned and are perpendicular to the orbital plane.

This presents a two part control problem. The first part is to reduce nutation by forcing ω_t equal to zero. The second part is maintaining the angle between the satellite's angular momentum vector H and the orbital angular momentum vector H_0 . The relationship between H and H_0 is

$$\cos \alpha = \frac{H_0 \cdot H}{|H_0| |H|}$$

The angle α can be obtained by precessing the satellite with control torques and then eliminating any resulting ω_t .

ω_t can be forced to zero by applying a control torque of magnitude equal to $I_t \omega_t$ in the direction of $I_t \omega_t$. ω_t can be calculated from measurements of ϕ , ψ , $\dot{\phi}$ and $\dot{\psi}$. The magnitude of torque required is determined by

$$F * r * dt = I_t \omega_t$$

where:

F = the impulsive force of the thruster

r = distance of the thruster from the center of mass

dt = time over which the thruster is fired.

An ideal thruster would provide an impulsive force at the correct time in the spin cycle and dt would be zero. The firing profile of an actual thruster can be approximated by the trapezoid model shown in Figure 5.1 [Ref. 3:p. 21]. t_1 is the time the thruster is commanded on, t_2 is the time the thruster reaches maximum force, t_4 is the time the thruster is commanded off and t_5 is the time the thruster force is zero. The total time dt is from t_1 to t_5 . t_c is the time at which the effective torque is applied.

t_2 and t_5 can be determined from experimental or the manufacturer's data. Knowing t_c , t_2 and t_5 , t_1 and t_4 can be determined by

$$\tan \lambda t_c = b/a \quad (5.1)$$

$$\frac{\omega t_c I_C}{r} = a \cos \lambda t_c + b \sin \lambda t_c \quad (5.2)$$

where:

$$a = \frac{\cos \lambda t_2 - \cos \lambda t_1}{\lambda(t_2 - t_1)} - \frac{\cos \lambda t_5 - \cos \lambda t_4}{\lambda(t_5 - t_4)}$$
$$b = \frac{\sin \lambda t_2 - \sin \lambda t_1}{\lambda(t_2 - t_1)} - \frac{\sin \lambda t_5 - \sin \lambda t_4}{\lambda(t_5 - t_4)}$$

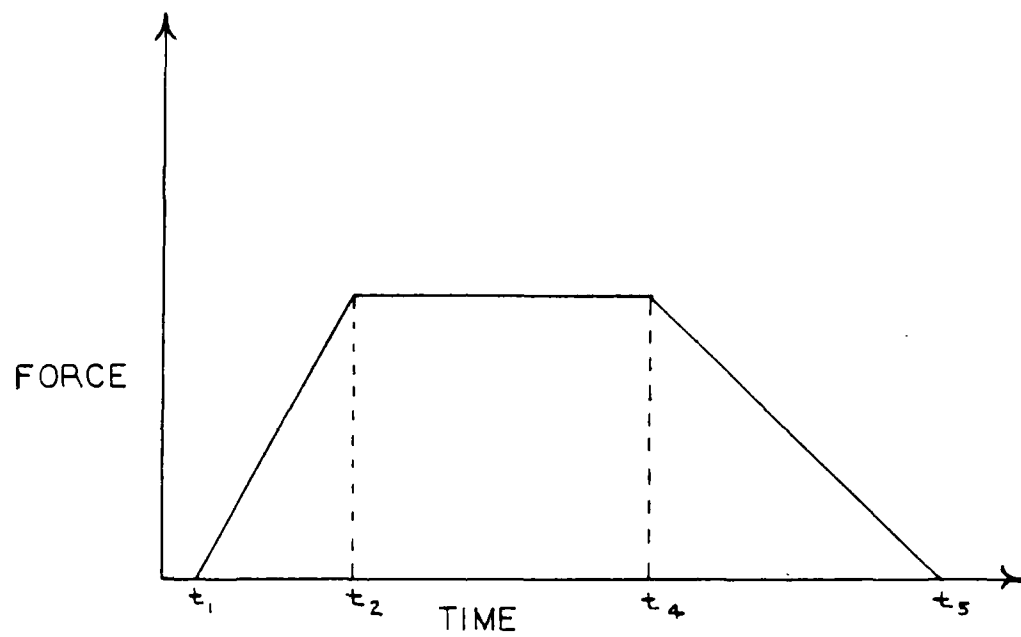


Figure 5.1 Typical Thruster Profile (Trapezoid Model)

Figure 5.2 shows the relationships between the firing profile and timing.

An even simpler approximation is the pulse function. This would occur if $t_2 = t_1$ and $t_4 = t_5$. Knowing that $dt = t_4 - t_2$, $t_c = (1/2)dt$. Therefore

$$t_2 = t_c - (1/2)dt \quad (5.3)$$

$$t_4 = t_c + (1/2)dt \quad (5.4)$$

Once the magnitude of control torque and the firing arc are known, the problem is when during the spin cycle to fire the thruster to eliminate ω_t . The acceleration of any point (x, y, z) on the satellite is

$$a_x = -x\omega_s^2 + \omega_n y A \sin \lambda t \quad (5.5)$$

$$a_y = (\omega_s - \lambda) A (z \cos \lambda t + x \sin \lambda t) \quad (5.6)$$

$$a_z = -z\omega_s^2 + \omega_n y A \cos \lambda t \quad (5.7)$$

where A is proportional to the nutation angle [Ref. 4:p. 116]. If an accelerometer is placed in the x - z plane, the axial acceleration reaches a positive peak when ω_t points towards the accelerometer. Placing a thruster 90 degrees from the accelerometer produces a torque opposite to ω_t . If the accelerometer is located on the z axis,

$$a_y = (\omega_s - \lambda) A z \cos \lambda t \quad (5.8)$$

and the peak acceleration is reached when $da_y/dt = 0$.

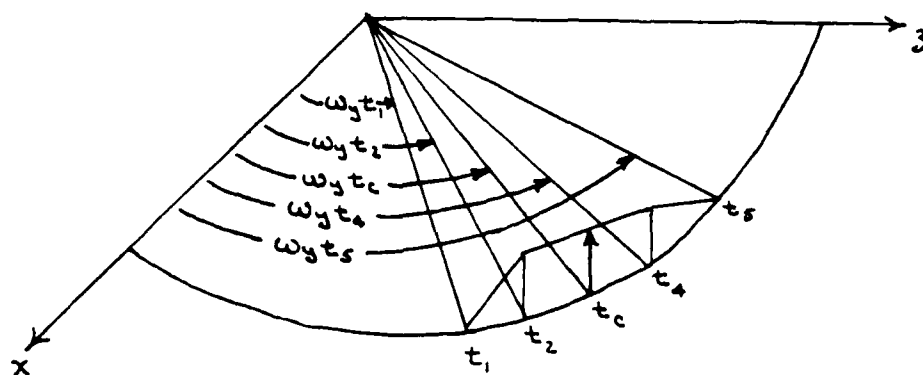


Figure 5.2 Relationship Between Spin Rate and Firing Times

Since

$$da_y/dt = -(\omega_s - \lambda)Az\lambda \sin \lambda t \quad (5.9)$$

then

$$da_y/dt = 0 \text{ when } t = \pi/\lambda$$

The value of acceleration at the firing point is

$$a_{y\max} = -(\omega_s - \lambda)zA \quad (5.10)$$

Using the value of $t = \pi/\lambda$ as t_c , the on and off times for the thruster can be calculated. If the spin rate is too fast, dt may encompass several revolutions of the satellite. To provide a torque in a given direction, however, the firing must be limited to an arc centered about t_c . Therefore, the total firing time required (dt) must be divided into segments occurring at integer multiples of t_c .

For example, assume the nutation angle is 1.0 deg (0.0174 rad), I_t is 8.91 kg-m², ω_y is -6.283 rad/sec, and H is 20.35 kg-m²/sec². Therefore

$$\begin{aligned} I_t \omega_t &= H \sin \eta \\ &= 0.355 \text{ kg-m}^2/\text{sec}^2 \end{aligned} \quad (5.11)$$

Assuming F is 0.448 n and R is 0.242 m

$$\begin{aligned} dt &= \frac{I_t \omega_t}{Fr} \\ &= 3.28 \text{ sec} . \end{aligned} \quad (5.12)$$

At 60 rpm the satellite makes one revolution per second. If the firing arc is 90 degrees, the firing time per arc is

$$\frac{\pi}{2\omega_y} = 0.25 \text{ sec} \quad (5.13)$$

Therefore, 13 firings will be required to eliminate the nutation. If the spin rate was 10 rpm, only 2 firings would be required. Each firing must occur at $a_{y\max}$ to avoid adding energy to the system.

This method of active nutation control was simulated using the computer model. Nutation was started by inputting a 5 n-m pulse of 0.01 seconds. After 0.03 seconds the control torque could be applied. The minimum required nutation was set at 0.001 radians to avoid computational errors. The firing arc was limited to 45 degrees.

To apply the correct control torque, the program calculated the value of a_y which would cause the acceleration peak to be in the center of the firing interval. When the calculated value of a_y was greater than this value, T_z was set equal to $2Fr/dt$ where dt is the firing arc time period. As long as the nutation was greater than 0.001, T_z was applied at the peak positive acceleration point.

This simulation was run for 3 different spin rates of 10, 20 and 60 rpm at an inertia ratio of 0.363. It was also run for two different inertia ratios and a constant spin rate. These results are shown in 3 series of 3 figures.

Each series shows the nutation angle and applied control torque, the ϕ and ψ angles and the firing diagrams for a different spin rate.

In Figure 5.3, the spin rate was 10 rpm. The initial nutation was 1.45×10^{-3} radians. It was reduced to 0.001 radians at 4.4 seconds. T_z was applied to reduce the nutation to 0.001 radians. From Figure 5.4, ϕ and ψ were reduced to steady-state values of 1.67×10^{-2} radians and -1.66×10^{-4} radians. The values of ϕ and ψ oscillated about these values because the nutation was not completely eliminated. Figure 5.5 shows the firing diagram for this case. T_z was 8.33×10^{-2} n-m over a firing time of .6 sec.

In Figure 5.6, the spin rate was changed to 20 rpm which resulted in an initial nutation of 7.28×10^{-3} . The first of 3 control firings occurred at 2.2 seconds. Nutation was reduced after 12 seconds. In Figure 5.7, the values of ϕ and ψ are 7.91×10^{-3} radians and -2.1×10^{-4} radians. From the firing diagram of Figure 5.8, T_z was 4.1×10^{-2} n-m over a pulse of .36 sec. Three pulses were needed for a total firing time of 1.08 seconds.

In Figure 5.9, a spin rate of 60 rpm was used. The initial nutation was 2.43×10^{-3} radians, the first application of control occurred at .7 seconds and the nutation was reduced after 27.5 seconds. ϕ and ψ from Figure 5.10 were 2.27×10^{-3} and -2.0×10^{-5} radians. From the firing diagram of Figure 5.11, 18 applications of T_z

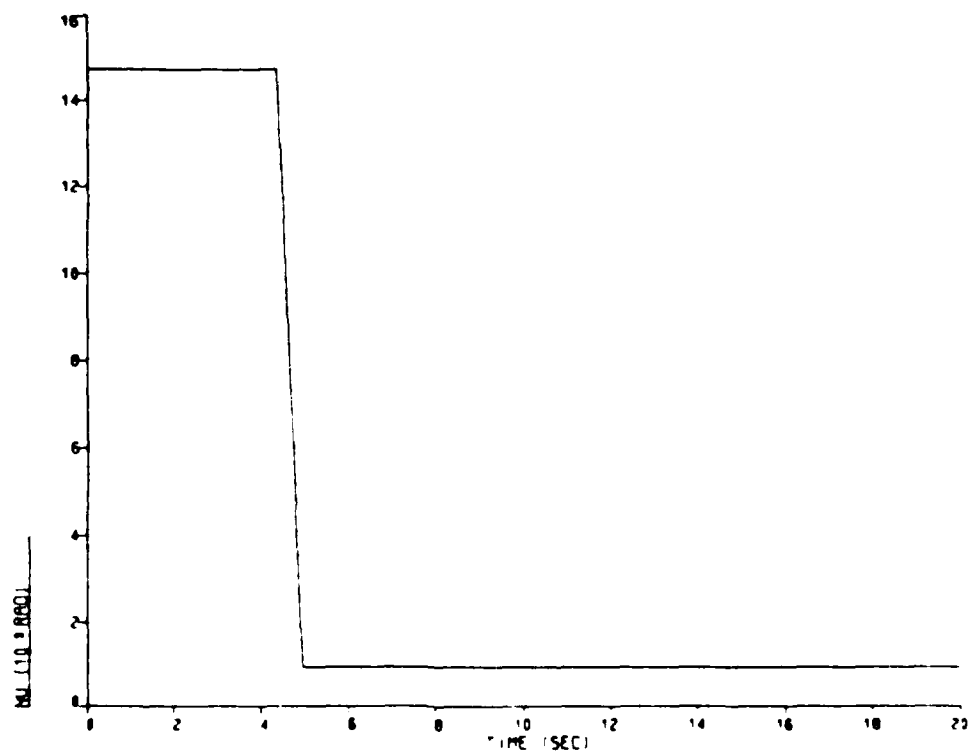


Figure 5.3 Mutation Control; $\omega_y = 10$ Rpm

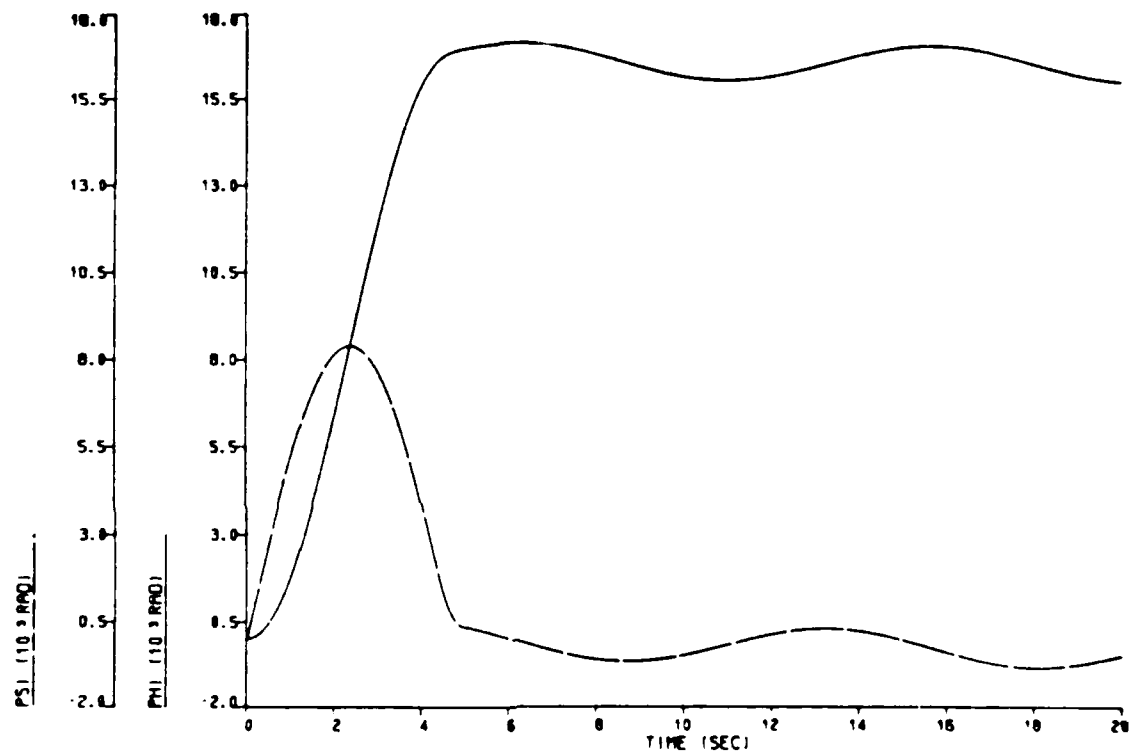


Figure 5.4 Roll and Yaw Angles; $\omega_y = 10$ Rpm

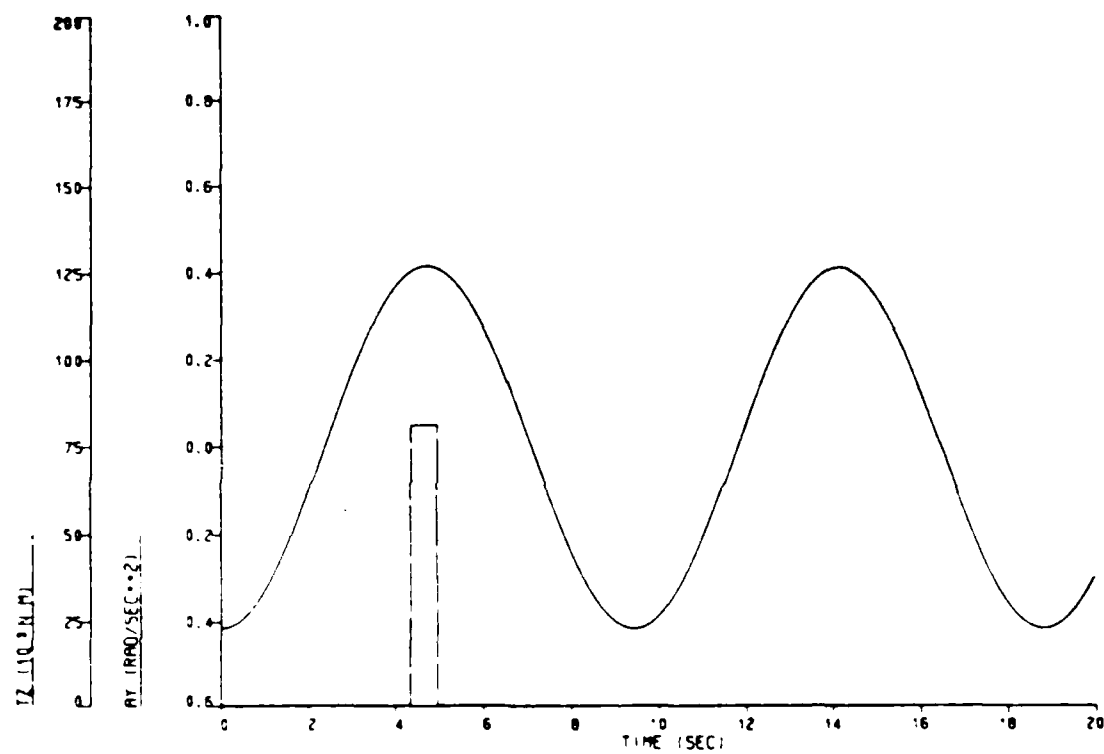


Figure 5.5 Firing Diagram; $\omega_y = 10$ Rpm

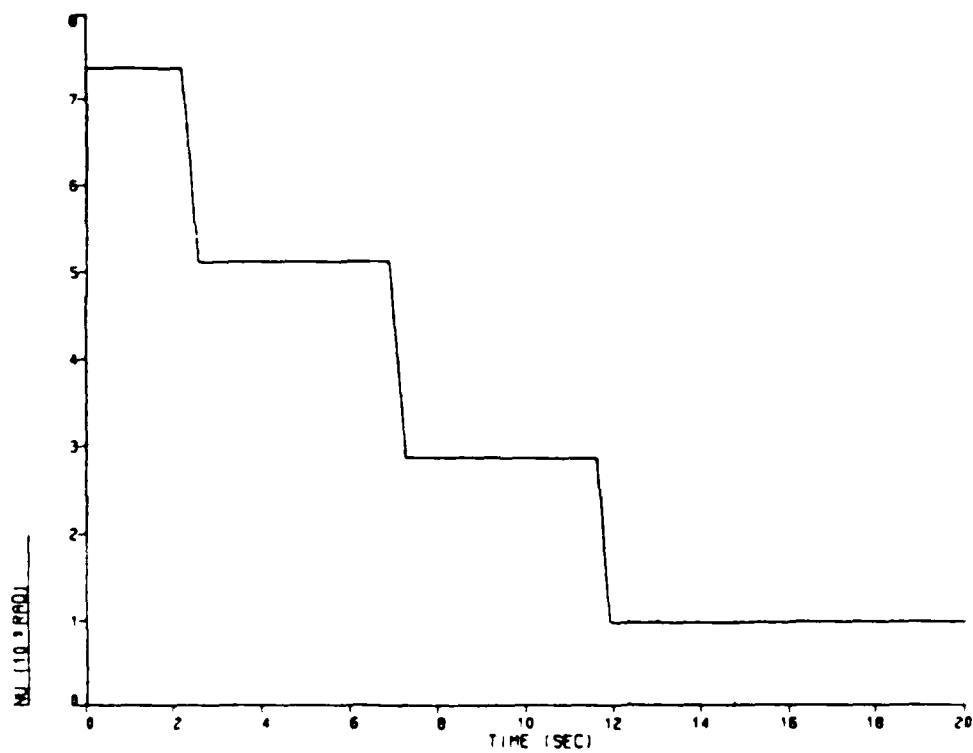


Figure 5.6 Nutation Control; $\omega_y = 20$ Rpm

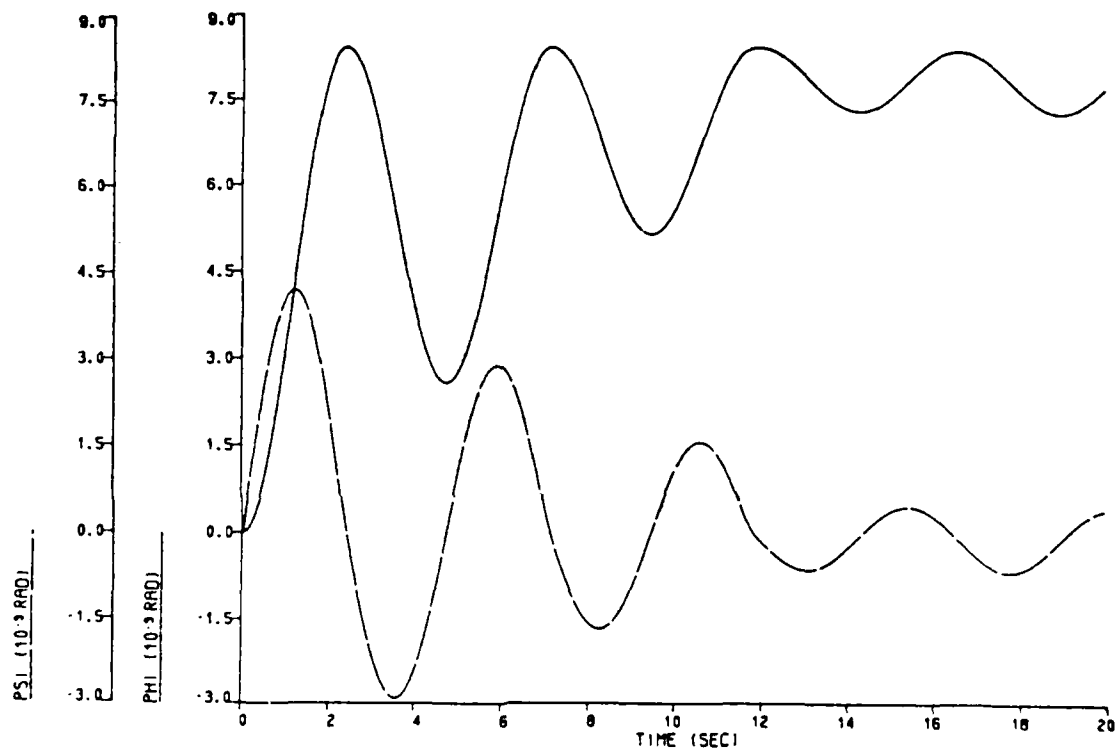


Figure 5.7 Roll and Yaw Angles; $\omega_y = 20$ Rpm

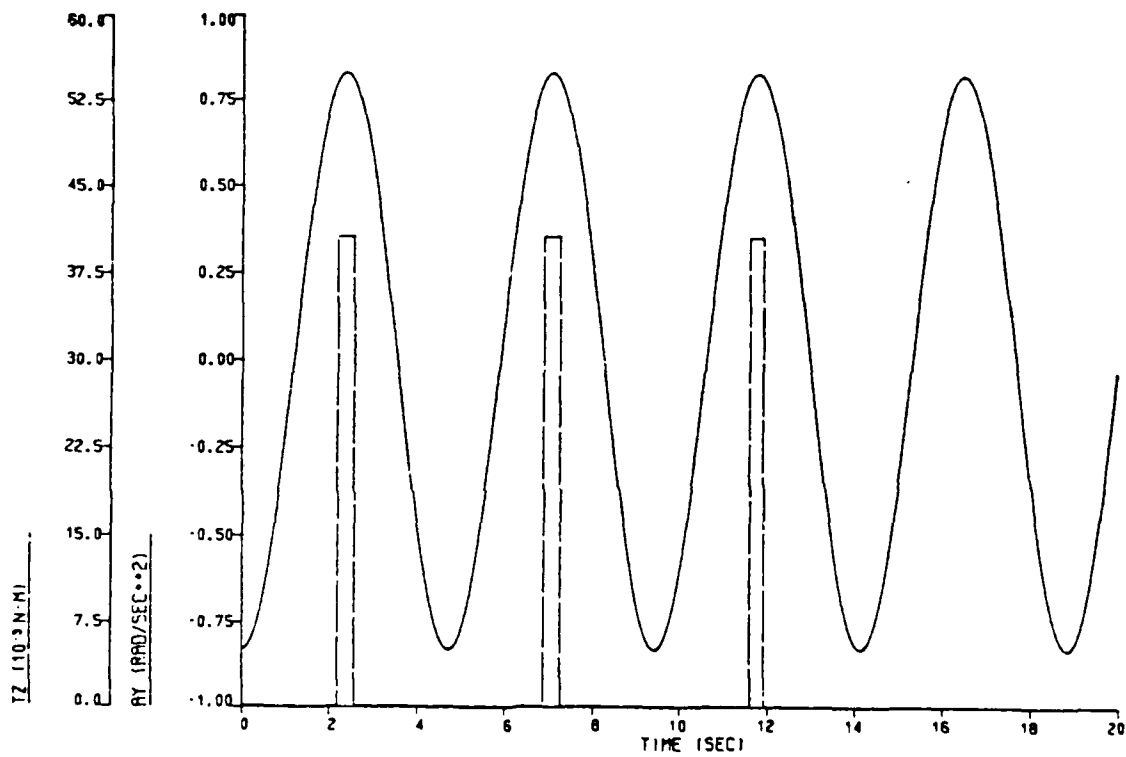


Figure 5.8 Firing Diagram; $\omega_y = 20$ Rpm

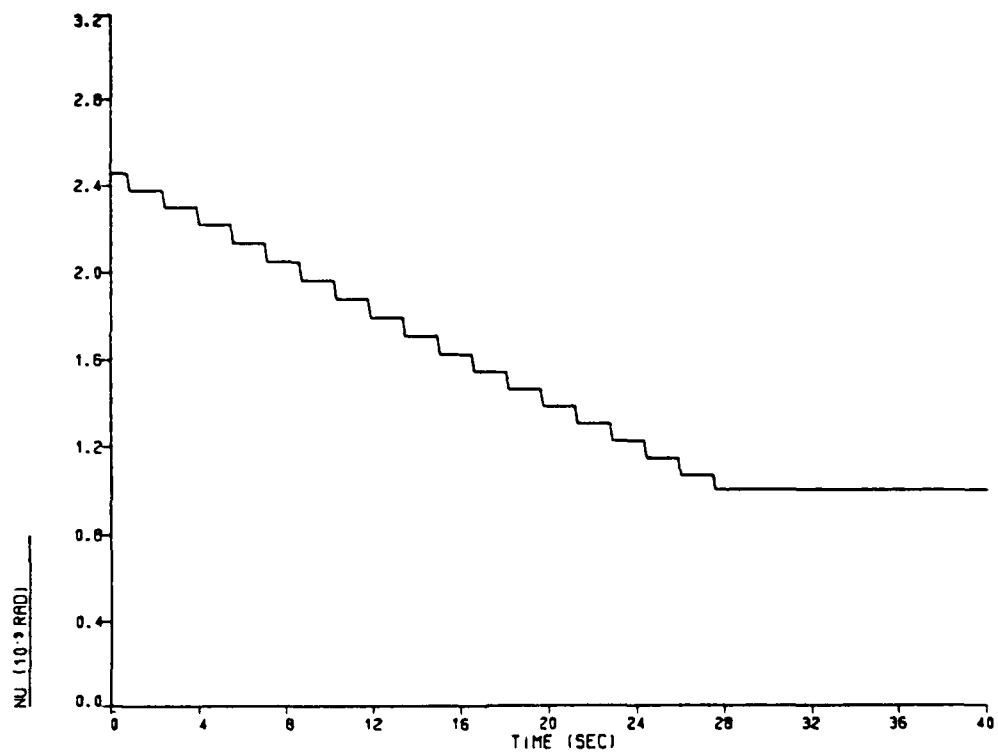


Figure 5.9 Nutation Control; $\omega_y = 60$ Rpm

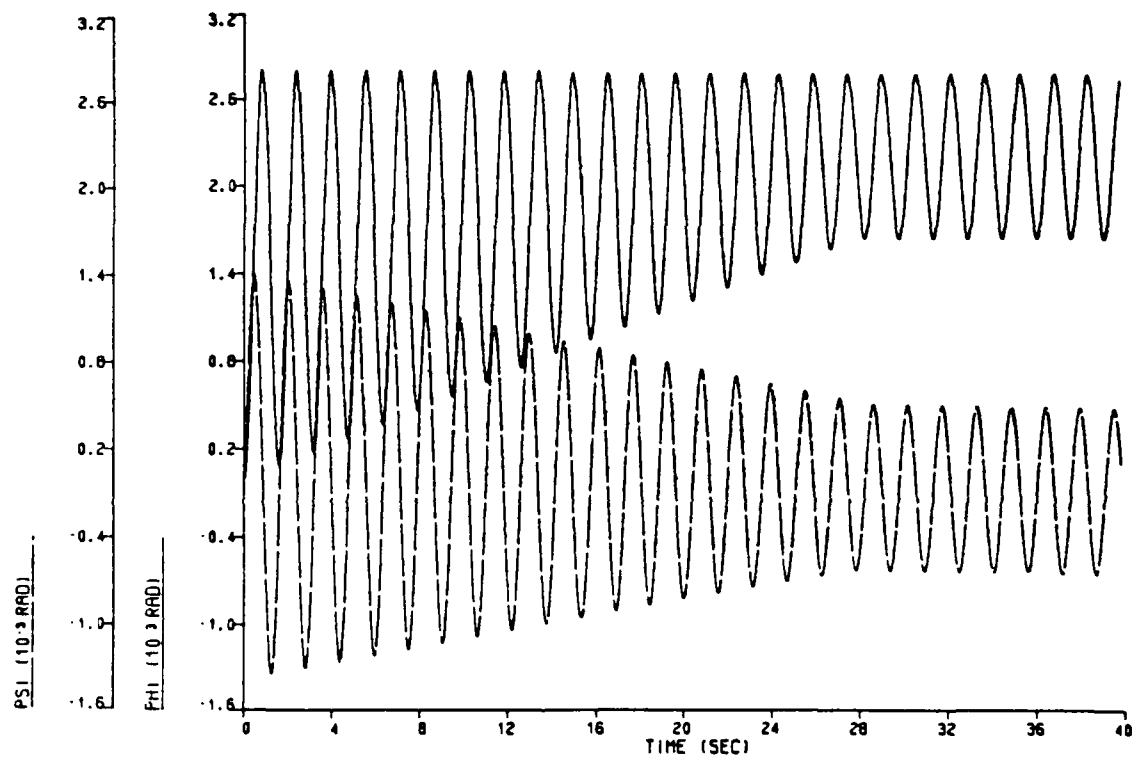


Figure 5.10 Roll and Yaw Angles; $\omega_y = 60$ Rpm

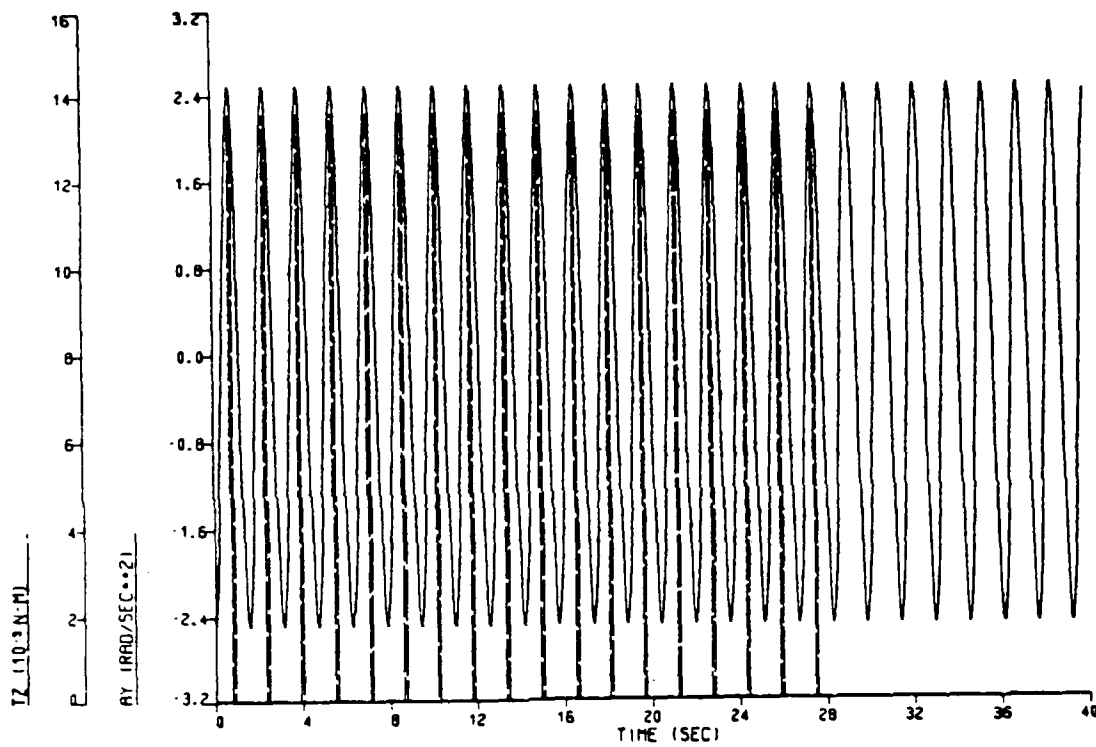


Figure 5.11 Firing Diagram; $\omega_y = 60$ Rpm

were required. T_2 was 1.3×10^{-2} n-m with a pulse width of .23 seconds. A total firing time of 4.2 seconds was required.

Figure 5.12 shows the difference in control for the same spin rate of 20 rpm but for two different inertia ratios. When $\sigma = 0.363$ it required 3 applications to reduce the nutation. When σ was increased to 1.12 the initial amount of nutation was less and only one application of control torque was required.

As a result of these simulations, it can be seen that the slower spin rates require less firing times and number of pulses. This is because the firing arc time is larger. A low number of pulses also reduces the probability of a timing error which may cause nutation instead of eliminate it. In every case shown, ϕ reached a steady state value while ψ approached zero. This is a result of using T_2 for the input and control torques.

Fewer pulses resulted in shorter firing times and quicker responses. This equates to a fuel savings. The model can also be run with different size thrusters by changing the value of F in the program. Larger firing arcs would also decrease the response times especially at higher spin rates.

B. SATELLITE REORIENTATION

The control system may be used to reorient the satellite as well as reduce the nutation. Reorientation can

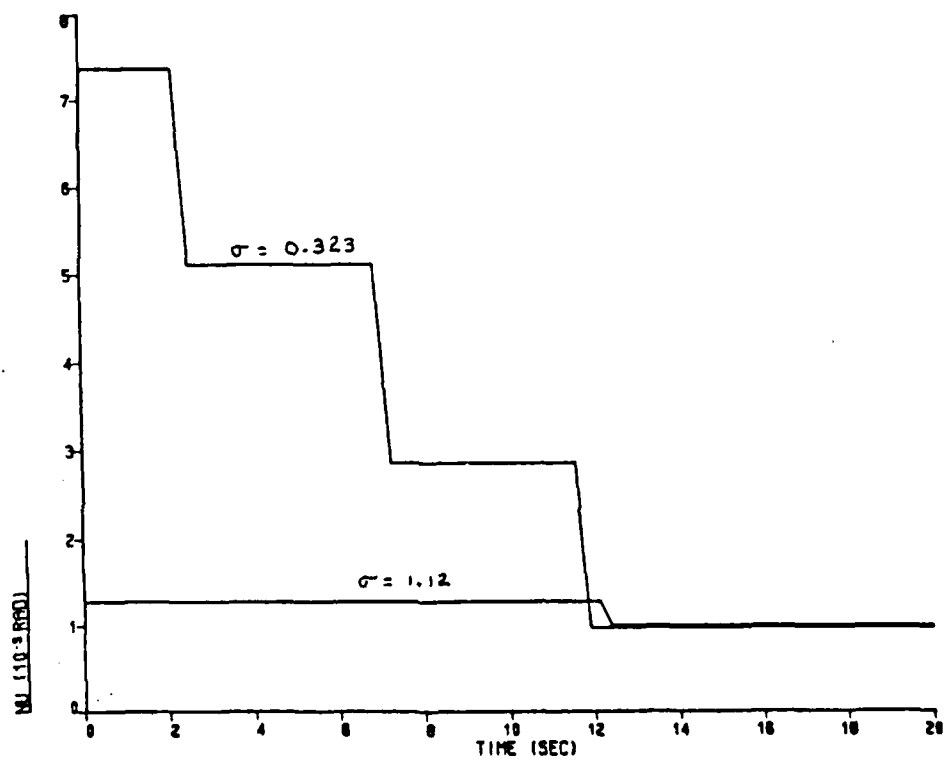


Figure 5.12 Nutation Variation with σ ; $\omega_y = 20$ Rpm

be accomplished either as part of the nutation reduction or as a separate control sequence. It was shown in Figures 5.4, 5.7 and 5.10 that although the nutation was reduced, ϕ and ψ were not returned to their initial values.

Reorientation during nutation control is a two-step process. The first step involves reducing the nutation angle by half its original amount. This will cause a new nutation cone to be established. When the spin axis moves 180° along the new cone, control torques are applied to reduce the nutation to the minimum level.

Because of the differences between nutation frequency, spin rate and λ , the thrusters may not be aligned with the ω_t vector when the satellite reaches the 180° point on the nutation cone. The time required for the spin axis to travel 180° is

$$\Delta t = \pi / \omega_n \quad (5.14)$$

The satellite will rotate about its axis through an angle

$$\alpha = \omega_y \Delta t \quad (5.15)$$

in this time period. The relative rotation of the ω_t vector is

$$\beta = \lambda \Delta t \quad (5.16)$$

over the same time period. The two angles α and β are equal only if $\sigma = 1.0$.

Figure 5.13 shows the relationship between ω_y , ω_n and λ .
 Since

$$\begin{aligned}\lambda &= (\sigma-1)\omega_y \\ &= (I_a/I_t - 1)\omega_y\end{aligned}\tag{5.17}$$

and

$$\omega_n = I_a/I_t \omega_y\tag{5.18}$$

The two angles α and β can be calculated as

$$\beta = \frac{\pi(\sigma-1)}{\phi}\tag{5.19}$$

$$\alpha = \pi/\sigma\tag{5.20}$$

Since over the required time period the thrust vector may not be aligned with the ω_t vector, the application of a control torque would add to the nutation.

To overcome this difficulty, four sets of thrusters can be used. If the thrusters are located on the x and z axes, a combination of thrusters can be fired to make the resulting torque collinear with the ω_t vector.

This is accomplished in the program by saving the time at which the nutation is halved as FTIME. When the program time reaches FTIME plus Δt , β is calculated and the correct combination of T_x and T_z used to reduce the nutation to an acceptable level and restore ϕ and ψ to their initial values.

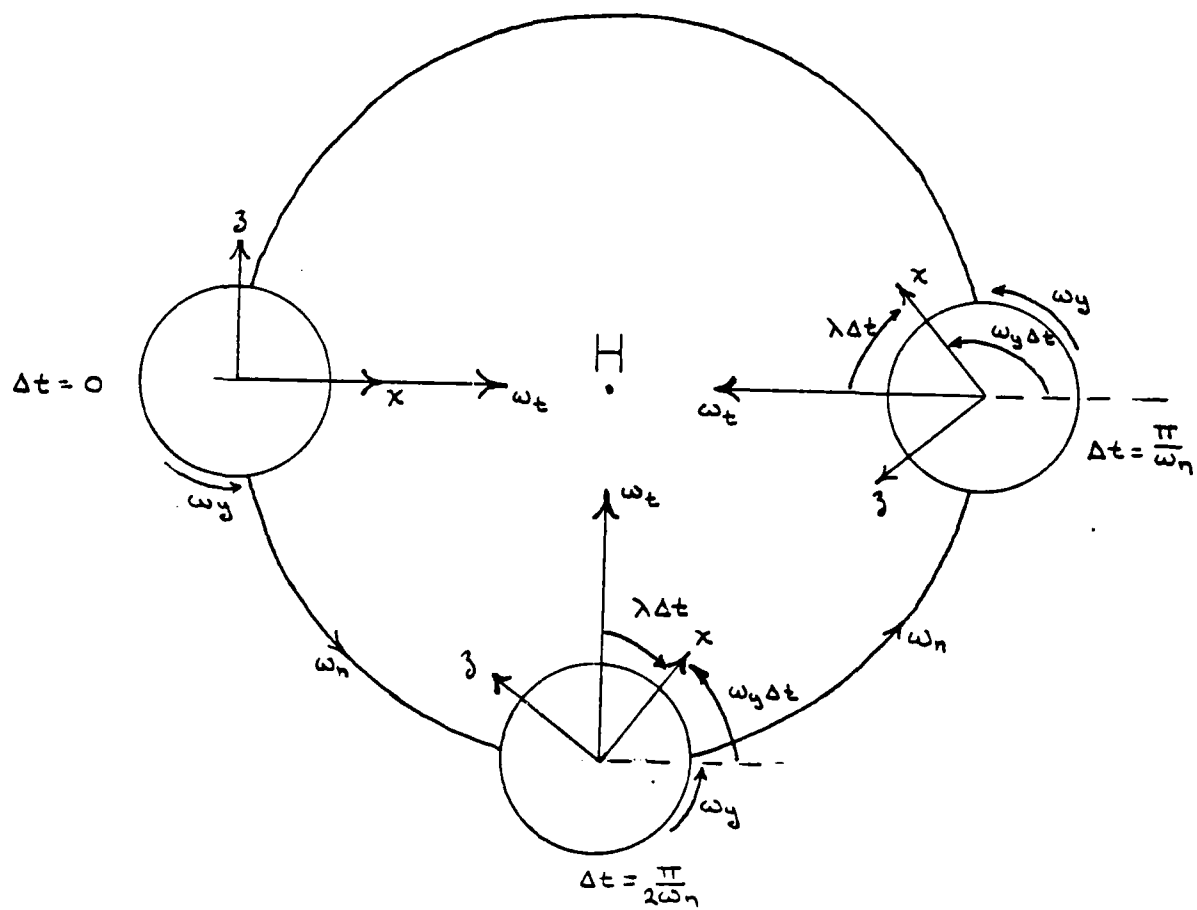


Figure 5.13 Relationship Between ω_y , λ , and ω_n

The second method is to reorient the satellite assuming there is no nutation. The degree of reorientation was given earlier in the chapter as

$$\cos \alpha = \frac{H_0 \cdot H}{|H_0| |H|}$$

Knowing the angle α and H_0 , the H required to make α zero can be calculated. This gives the required ω_t . A control torque equal to $I_t \omega_t$ is applied to start the satellite nutating. When Δt is equal to π/ω_n a control torque equal and opposite to $I_t \omega_t$ is applied to reduce the nutation. This is done in a manner similar to that of reorienting the satellite with nutation.

VI. CONCLUSIONS

This thesis derived the equations which describe the rotational motion of a satellite. It also derived the equations describing the effects of gravity gradient torque and aerodynamic drag. These equations were then used to construct a computer simulation model. The model was used to analyze how changes in moments of inertia and spin rates affect the motion of the satellite.

It was shown that extending magnetometers on booms would cause I_a and I_t to increase. This changed the inertia ratio σ . The spin rate of the satellite could then be changed by changing the boom length of the magnetometer. As σ increased, the stability of the satellite was changed. A high value of σ made the satellite resistive to nutation by external forces.

The effects of gravity gradient and aerodynamic drag were analyzed. The amount of nutation caused by environment depended on the spin rate and σ . The maximum amount of nutation occurs at a low spin rate and low σ . The nutation is on the order of 2.053×10^{-3} radians for a σ of 0.363 and a 10 rpm spin rate. The effects of the environment need only to be taken into account in the motion analysis if the accuracy required by the control system is small. The accuracy for ORION is to be within 2 degrees so gravity

gradient and drag were only applied during the example flight profile.

The control system that is used is an active nutation control. An example of how the control system would be used was given. Assuming a firing arc of 45° , 4.4 seconds were required to reduce the nutation at a spin rate of 10 rpm, 12 seconds for a spin rate of 20 rpm and 27.5 seconds for a spin rate of 60 rpm. The procedure for reorienting the satellite to any desired attitude was also described.

Although the computer model was written to simulate the satellite as closely as possible, many areas need more detailed modelling. The satellite was assumed to be a cylinder of uniform mass. The actual mass distribution needs to be determined and the moments of inertia calculated. This would change the inertia ratio and possibly cause some cross-products of inertia to develop.

Another factor that was not included in this model is the effect of liquids slosh in the fuel tanks. This could cause internal torques that adversely affect the motion. These tanks could also be designed to dissipate energy. If this could be done, then when σ was greater than one, the satellite could be made stable.

The firing profile of the control thruster was assumed in the model to be a pulse function. Entering the profile as a trapezoid would increase the accuracy of the model.

When real thruster data becomes available it could then be entered.

As has been stated before, many of the variables in the program can easily be changed in parameter runs. This allows a great deal of flexibility in analyzing design changes as they occur.

APPENDIX

ATTITUDE ANGLE CONTROL PROGRAM

TITLE ATTITUDE ANGLE CONTROL PROGRAM
 * THIS PROGRAM PROVIDES THE SIMULATION MODEL FOR THE CONTROL OF THE
 * ORION SATELLITE. IT USES THE EQUATIONS DERIVED IN CHAPTER 3 TO MODEL
 * SATELLITE MOTION AND ENVIRONMENTAL TORQUES. IT CALCULATES THE ANGULAR
 * FREQUENCIES AND THE ATTITUDE ANGLES. IT CALCULATES THE MAGNITUDE OF
 * THE ENVIRONMENTAL TORQUES BASED ON ORBITAL PARAMETERS. IT ALSO
 * COMPUTES THE NUTATION, ANGULAR MOMENTUM VECTOR AND THE CONTROL TORQUES
 * NECESSARY FOR THE ACTIVE NUTATION CONTROL SYSTEM. CHANGES TO THE
 * PROGRAM CAN BE MADE VIA PARAM STATEMENTS OR DIRECTLY IN THE LISTING.

* VARIABLE DESCRIPTION

* L = DISTANCE FROM THE CENTER OF PRESSURE TO THE CENTER OF MASS
 * F = THRUST FORCE OF ONE CONTROL THRUSTER
 * R = RADIUS OF THE SATELLITE
 * IT = TRANSVERSE MOMENT OF INERTIA
 * IA = MOMENT OF INERTIA ALONG THE SPIN AXIS
 * ALT = ORBITAL ALTITUDE OF THE SATELLITE
 * RO = RADIUS OF THE EARTH
 * ROE = DENSITY OF AIR AT THE ORBITAL ALTITUDE
 * WO = ANGULAR VELOCITY OF THE SATELLITE WRT EARTH
 * D = DRAG FORCE
 * WX = ANGULAR VELOCITY ABOUT THE X AXIS WRT EARTH
 * WZ = ANGULAR VELOCITY ABOUT THE Z AXIS WRT EARTH
 * WY = ANGULAR VELOCITY ABOUT THE Y AXIS WRT EARTH
 * PHID = SATELLITE ROTATION ABOUT THE X AXIS
 * PSID = SATELLITE ROTATION ABOUT THE Z AXIS
 * THD = SATELLITE ROTATION ABOUT THE Y AXIS
 * PHI = ROLL ANGLE
 * PSI = YAW ANGLE
 * TH = PITCH ANGLE
 * TDx = DRAG TORQUE IN THE X DIRECTION
 * TDZ = DRAG TORQUE IN THE Z DIRECTION
 * TD = TOTAL DRAG TORQUE
 * GX = GRAVITY GRADIENT IN THE X DIRECTION
 * GZ = GRAVITY GRADIENT IN THE Z DIRECTION
 * GG = TOTAL GRAVITY GRADIENT TORQUE
 * TX = CONTROL TORQUE IN THE X DIRECTION
 * TZ = CONTROL TORQUE IN THE Z DIRECTION
 * TY = CONTROL TORQUE IN THE Y DIRECTION
 * WT = TRANSVERSE ANGULAR VELOCITY
 * HT = TRANSVERSE COMPONENT OF THE ANGULAR MOMENTUM VECTOR
 * HS = AXIAL COMPONENT OF THE ANGULAR MOMENTUM VECTOR
 * H = MAGNITUDE OF THE ANGULAR MOMENTUM VECTOR
 * NU = NUTATION ANGLE
 * SIGMA = INERTIA RATIO
 * LAMDA = RELATIVE VELOCITY OF WT WRT THE SATELLITE ROTATION
 * WH = NUTATION FREQUENCY WRT INERTIAL SPACE
 * AY = AXIAL ACCELERATION OF THE SATELLITE DURING NUTATION
 * FARC = FIRING ARC OF THE CONTROL THRUSTERS
 * TC = TIME OF PEAK POSITIVE AXIAL ACCELERATION
 * AON = ACCELERATION AT THE THRUSTER TURN ON TIME
 * FTIME = TIME OF THE THRUSTER FIRING
 * CANCEL = TIME FOR THE SPIN AXIS TO TRAVEL 360 DEGREES

CONST IT=8.911, IA=3.239, R=0.242, F=0.44

METHOD RK4FX

FIXED FLAG

INTEGER

* INITIAL PROGRAM STATEMENTS: SPIN

INIT

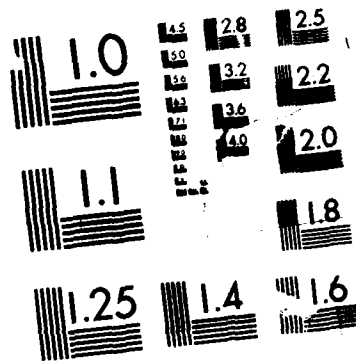
AD-A187 179

PRELIMINARY DESIGN OF THE ORION ATTITUDE CONTROL SYSTEM 2/2
(U) NAVAL POSTGRADUATE SCHOOL MONTEREY CA D C CHAPPELL
DEC 87

UNCLASSIFIED

F/G 22/2 NL





MICROCOPY RESOLUTION TEST CHART
NATIONAL BUREAU OF STANDARDS-1963-A

```

      ALT = 200.00
      ROE = 7.0D-10
      RO = (6378.0+ALT)*1.0D03
      WO = SQRT(3.987D14/RO**3)
      D = 1.7D14*ROE/RO
      FLAG = 0
INCON W XO=0.0, WZO=0.0, WYO=-2.093, PHIO=0.0, PSIO=0.0, THO=0.0
DERIV
      WXD = (TX+TDX+GX-(IT-IA)*WY*WZ)/IT
      WZD = (TZ+TDZ+GZ-(IA-IT)*WY*WX)/IT
      WYD = TY/IA
      PHID = WX + PSI*WO
      PSID = WZ-PHI*WO
      THD = WY+WO
      WX = INTGRL(WXO, WXD)
      WZ = INTGRL(WZO, WZD)
      WY = INTGRL(WYO, WYD)
      PHI = INTGRL(PHIO, PHID)
      PSI = INTGRL(PSIO, PSID)
      TH = INTGRL(THO, THD)
DYNAMIC
* ENVIRONMENTAL TORQUE CALCULATION; USE WHEN DISTURBANCE TORQUES ARE
* REQUIRED
*   TDX = -D*L*SIN(TH)*COS(PSI)
*   TDZ = D*L*COS(TH)*COS(PSI)
*   ID = (TDX**2+TDZ**2)**0.5
*   GX = 3.0*(WO**2)*(IT-IA)*SIN(PHI)*COS(PHI)*(COS(TH))**2
*   GZ = 3.0*(WO**2)*(IT-IA)*SIN(TH)*COS(TH)*SIN(PHI)
*   GG = (GX**2+GZ**2)**0.5
*****
* USE THE NEXT 4 STATEMENTS WHEN NO DISTURBANCE TORQUES ARE REQUIRED
      TDX = 0.0
      TDZ = 0.0
      GX = 0.0
      GZ = 0.0
*****
      TX = 0.0
      TY = 0.0
*
* STEP FUNCTION USED TO SET AN INITIAL NUTATION VALUE
      TZ = 5.0*STEP(0.01)-5.0*STEP(0.02)
*
* CALCULATION OF ANGULAR VELOCITIES, MOMENTUM VECTORS AND FREQUENCIES
      WT = (WX**2 + WZ**2)**0.5
      HT = IT*WT
      HS = IA*WY
      H = (HT**2 + HS**2)**0.5
      NU = ARSIN(HT/H)
      SIGMA = IA/IT
      LAMDA = (SIGMA-1.0)*WY
      WN = SIGMA*WY
*
* CALCULATION OF THE FIRING TIME AND FIRING ARC
      AY = (WY-LAMDA) * R * COS(LAMDA*TIME)
      FARC = 0.392699/ABS(WY)
      TC = 3.14159/LAMDA
      AON = (WY-LAMDA)*R*COS(LAMDA*(TC-FARC))
*
* THIS STATEMENT ALLOWS THE NUTATION TO BE PRESENT BEFORE CONTROL OCCURS
      IF (TIME.LE.0.2) GO TO 15
*
* CONTROL CALCULATION AND FIRING. IF FLAG IS 0 THE CONTROL SYSTEM WILL
* REDUCE THE INITIAL NUTATION BY HALF THEN FIRE TO REDUCE THE ATTITUDE
* ANGLES TO ZERO. IF THE FLAG IS 1 THE CONTROL SYSTEM WILL REDUCE THE
* NUTATION TO NUREF ONLY.
      IF((NU-NUREF).LE.0.00001) THEN
          TX = 0.0
          TZ = 0.00000
      ELSE
          IF(FLAG.EQ.0) THEN

```

```

      DNU = (NU-NUREF)/2.0 + NUREF
      FLAG = 1
    END IF
    IF (AY.GT.AON.AND.FLAG.EQ.1) THEN
      FTIME = TIME
      TZ = 2.0*F*R*FARC
      TX = 0.0
    ELSE
      TZ=0.0
      TX=0.0
    END IF
    IF (NU.LE.DNU) THEN
      CANCEL = FTIME + ABS(3.14159/WN)
      FLAG = 2
    END IF
* CALCULATION OF THE CORRECT THRUSTER COMBINATION REQUIRED TO REDUCE
* THE ATTITUDE ANGLES TO A MINIMUM.
    IF (TIME.GE.CANCEL.AND.FLAG.EQ.2) THEN
      DT = CANCEL + 2*FARC
      CONT = 4*F*R*FARC
      TCL = -CONT*STEP(CANCEL) + CONT*STEP(DT)
      IF (SIGMA.GT.1.0) THEN
        BETA = ((SIGMA-1.0)*3.14159/SIGMA) -6.283
      ELSE
        BETA = (SIGMA-1.0)*3.14159/SIGMA
      END IF
      IF (BETA.GT.0.0.OR.BETA.LE.-1.5708) THEN
        DELTA = ABS(BETA)
        TZ = -TCL*COS(DELTA)
        TX = -TCL*SIN(DELTA)
      ELSEIF (BETA.GT.-1.5708.OR.BETA.LE.-3.14159) THEN
        DELTA = 3.14159- ABS(BETA)
        TZ = TCL*COS(DELTA)
        TX = -TCL*SIN(DELTA)
      ELSEIF (BETA.GT.-3.14159.OR.BETA.LE.-4.7123) THEN
        DELTA = ABS(BETA) - 3.14159
        TZ = TCL*COS(DELTA)
        TX = TCL*SIN(DELTA)
      ELSEIF (BETA.GT.-4.7123.OR.BETA.LE.-6.283) THEN
        DELTA = 6.283 - ABS(BETA)
        TZ = -TCL*COS(DELTA)
        TX = TCL*SIN(DELTA)
      END IF
    END IF
15  END IF
    CONTRL FINTIM=20.0, DELT=0.01
    SAVE .01, NU, PHI, PSI, WX, WZ, WY, SIGMA, LAMDA, WN, AY, AON, ...
      H, HS, HT, PHID, PSID, THD, TH, TX, TY, TZ, WT
    GRAPH (G1,DE=TEK618) TIME(UN=SEC) PHI(UN=RAD,LO=-3.0E-03,SC=1.5E-03)...
      PSI(UN=RAD,LO=-3.0E-03,SC=1.5E-03)
    GRAPH (G3,DE=TEK618) TIME NU(UN=RADS)
    GRAPH (G4,DE=TEK618) TIME TX TZ(LO=-32E-03,SC=.0165)
    LABEL (G1,DE=TEK618) ROLL AND YAW ANGLES; WY = 20RPM
    LABEL (G2,DE=TEK618) YAW ANGLE; SIGMA=0.3635 & 1.479; WY=-6.283
    LABEL (G3,G9,DE=TEK618) NUTATION ANGLE; WY = 20 RPM
    LABEL (G4,DE=TEK618) FIRING DIAGRAM WY = 20 RPM
    END
    STOP

```

LIST OF REFERENCES

1. Boyd, Austin, W., Fuhs, Allen E., "General Purpose Satellites: A Concept for Affordable Low Earth Vehicles," Paper presented at AIAA 25th Aerospace Sciences Meeting Reno, Nevada, 12 January 1987.
2. USAF Airforce System Command Space Planners Guide.
3. Wertz, James R. (Ed.), Spacecraft Attitude Determination and Control, D. Reidel Publishing Company, 1984.
4. Agrawal, Brij N., Design of Geosynchronous Spacecraft, Prentice-Hall Inc., 1986.
5. Hughes, Peter C., Spacecraft Attitude Dynamics, John Wiley and Sons, 1986.

INITIAL DISTRIBUTION LIST

	No. Copies
1. Defense Technical Information Center Cameron Station Alexandria, Virginia 22304-6145	2
2. Library, Code 0142 Naval Postgraduate School Monterey, California 93943-5002	2
3. Chairman, Code 62 Department of Electrical and Computer Engineering Naval Postgraduate School Monterey, California 93943-5004	1
4. Commander United States Space Command Attn: Technical Library Peterson AFB, Colorado 80914	1
5. LT David C. Chappell Naval Electronic System Engineering Center Bldg 509 Marine Island Vallejo, California 94592	1
6. Dr. George Thaler, Code 62Th Naval Postgraduate School Monterey, California 93943-5000	1
7. Dr. Allen E. Fuhs Distinguished Professor (Emeritus) 25932 Carmel Knolls Carmel, California 93923	2
8. Mr. Marty Mosler Naval Postgraduate School Monterey, California 93943-5000	1
9. Commander Naval Space Command Attn: Code N3 Dahlgren, Virginia 22448-5170	1

END

FEB.

1988

DTic